Multiphoton exciton absorption in a semiconductor superlattice in a dc electric field

B. S. Monozon[1] and P. Schmelcher[1,2]
[1]*Theoretische Chemie, Institut für Physikalische Chemie, Universität Heidelberg, INF 229, 69120 Heidelberg, Germany*
[2]*Physikalisches Institut, Universität Heidelberg, Philosophenweg 12, 69120 Heidelberg, Germany*
(Received 18 July 2006; revised manuscript received 19 December 2006; published 15 June 2007)

An analytical approach to the problem of the multiphoton exciton absorption in biased narrow-well superlattices (SLs) induced by the optical transitions to the localized resonant exciton states is developed. Both the ac electric field of the intense optical wave and the dc electric field are directed parallel to the SL axis. The SL is formed by a periodic sequence of quantum wells (QWs) whose widths are taken to be much less than the exciton Bohr radius. The model of the SL potential employs a limiting form of the Kronig-Penney potential, i.e., a periodic chain of QWs separated by δ-function-type barriers. A sufficiently strong dc electric field provides the localization of the carriers within one period of the SL. Analytical dependencies of the coefficient of the multiphoton exciton absorption on the characteristics of the dc and ac electric fields and on the parameters of the SL in the approximation of both isolated and interacting Wannier-Stark levels are obtained in the nearest-neighbor tight-binding approximations. Our analytical results correlate well with those obtained in numerical investigations. Estimates of the expected experimental values are performed for the parameters of a GaAs/AlGaAs SL.

DOI: 10.1103/PhysRevB.75.245207 PACS number(s): 71.35.−y, 73.21.Cd, 71.35.Cc

I. INTRODUCTION

Since the pioneering papers of Bloch[1] and Wannier,[2] electronic and optical effects in a semiconductor superlattice (SL) exposed to external electric fields attracted much attention both theoretically and experimentally. Electrons subjected to a time-independent (dc) electric field E directed parallel to the axis of the SL with period d exhibit Bloch oscillations within the spatial region $\Delta/2eE$ (Δ is the miniband width). The energies of these spatially localized states are the Wannier-Stark levels (WSLs) with the distance eEd between the neighboring levels. If the dc field is replaced by a time-dependent (ac) electric field $F_0 \cos \omega t$ of strength F_0 and frequency ω, the dynamic localization occurs if the condition $J_0(eF_0d/\hbar\omega)=0$ is obeyed [$J_n(x)$ are the Bessel functions].[3] In the presence of combined dc-ac electric fields $E+F_0 \cos \omega t$, the conditions of the localization become $eEd/\hbar\omega=n=0,1,2,\ldots$; $J_n(eF_0d/\hbar\omega)=0$.[4–6] Numerous experimental and theoretical investigations on fascinating phenomena such as absolute negative conductance, phonon-assisted transport, dynamic Franz-Keldysh effect, terahertz (THz) radiation, and THz photocurrent resonance and chaotic scattering have been performed (see Refs. 7 and 8 and references therein).

By the present time, excitonic effects caused by the Coulomb interaction between the electron (e) and hole (h) have been observed for the majority of low-dimensional structures based on the III-V and II-VI semiconductors. Clearly, excitons strongly modify the electronic and optical properties of the SLs. A study of the one-photon exciton effects was developed originally in biased SLs in Refs. 9–14 and then successfully continued in more recent works[15–18] devoted to excitons in SLs in the presence of combined dc-ac electric fields.

In the majority of experimental and theoretical studies the biased GaAs/$Al_{0.3}Ga_{0.7}$As SLs of well width $d_w \simeq 35-65$ Å, period $d \simeq 50-90$ Å, and miniband width $\Delta \simeq 10-90$ meV subjected to dc electric fields $E \simeq 10-50$ kV/cm have been considered.[8,17–22] These SLs consist of the narrow quantum wells (QWs) of width d_w being less than the Bohr radius of the exciton in the GaAs material, $a_0 \simeq 100$ Å. One of the reasons for consideration of these SLs is that a narrow QW causes the quasi-two-dimensional (quasi-2D) exciton to be more stable. In units of the effective exciton Rydberg constant Ry, the binding energy $\mathcal{E}_b$ of the 2D exciton is 4 Ry compared to $\mathcal{E}_b=1$ Ry for the bulk material. We consider the cases of (a) relatively weak dc electric fields $E<E_0$ ($E_0=\Delta/2ed$) and the carriers being spatially distributed between several periods of the SL and (b) strong fields $E>E_0$ providing the localization of the carriers within one period (see Refs. 9 and 10 and those listed in Table I). For the latter electric fields, the exciton Rydberg constant Ry $\simeq 4.7$ meV is less than the distance between neighboring WSLs $eEd \simeq 10-30$ meV. As a result, the exciton energy spectrum in the GaAs/AlGaAs SL is a sequence of Rydberg series consisting of quasidiscrete states each being adjacent to the WSL from the low-energy side and being in resonance with states of the continuous spectrum branching from the lower WSLs.[19,20,23,24] One-photon absorption of the probing weak light with optical frequencies $\hbar\omega \geqslant 10^3$ meV is a widespread tool to study quasienergetic exciton states in biased SLs.[8,21,22,25] Two- and three-photon spectroscopy of the GaAs/AlGaAs,[26] ZnSe/ZnSSe,[27–29] and ZnCdSe/ZnSe (Ref. 30) SLs has been only performed in the absence of dc electric fields. The absolute majority of the theoretical investigations of exciton states and exciton absorption in SLs subjected to combined dc-ac electric fields are based on numerical techniques, which employ semiconductor Bloch equations,[31] dynamics controlled truncation theory,[32] and the excitonic basis.[15,18,33] Numerical approaches are indispensable for a detailed comparison with experimental data. Analytical methods applied and/or developed in the present work are complementary in the sense that they provide the possibility to follow the evolution of the exciton spectrum as a

function of the parameters of the SL and characteristics of the dc-ac electric fields.

In order to fill the above indicated gap, we develop an analytical approach to the problem of multiphoton absorption in biased narrow-well SL induced by optical transitions to the localized resonant exciton states. It emphasizes the basic physics of the unique quasienergetic Wannier-Stark states and suggests further experiments related to the nonlinear optical exciton absorption in biased SLs. We consider the case where both the ac field ($F_0 \cos \omega t$) of the intense optical wave and the dc (E) electric field are directed parallel to the axis of the SL that, in turn, is modeled by a limiting form of the Kronig-Penney potential consisting of a periodic chain of the QWs of width $d_w = d$ separated by the δ-function-type barriers. The exciton Bohr radius a_0 considerably exceeds the width d of the QWs. The dc electric field is taken to be strong ($E \gg \Delta/2ed$) to localize the carriers within the period of the SL. The complete exciton wave function is then expanded with respect to the basis formed by the longitudinal one-dimensional quasienergetic Wannier-Stark wave functions of the electron-hole pair in the SL in the presence of combined dc-ac electric fields. The set of the equations for the transverse radial quasi-Coulomb wave functions describing the motion in the heteroplanes is solved in the approximation of two interacting WSLs (double-WSL approximation) to give, in turn, the complex energies of the resonant exciton states. The positions and finite widths of the peaks of multiphoton absorption associated with the dipole optical transitions to the resonant quasienergetic exciton states are calculated in explicit form. Analytical dependencies of the coefficient of the multiphoton exciton absorption on the frequency ω and magnitude F_0 of the electric field of the light, on the strength of the dc electric field E, and on the parameters of the SL (miniband width Δ and period d) are obtained.

It is shown that the spectrum of the optical absorption in the narrow-well SL associated with the transitions to the spatially localized exciton states consists of a sequence of quasi-2D quasi-Rydberg series of resonances with each series being adjusted to the specific electron-hole WSL of index σ. The ground exciton peak dominates in each exciton series. The most intense series of the one-photon absorption is associated with the WSL $\sigma = 0$, while considerably less intense series correspond to the WSLs with $\sigma = \pm 1$. The most intense series of the multiphoton absorption are those relevant to the WSLs $\sigma = \pm 1$, with the even-photon spectrum containing the additional, significantly less intense, series adjacent to the WSL $\sigma = 0$. With increasing dc electric field, the exciton absorption increases. The greater the miniband widths Δ_{eh} and the greater the magnitude of the ac electric field F_0 are, the stronger the multiphoton absorption is. Increasing the dc electric field and decreasing the QWs width lead to a decrease in efficiency of the coupling between the neighboring WSLs that, in turn, leads to the exciton states becoming more stable.

Our analytical results are in line with those obtained numerically.[11,20,46] Estimates of the expected experimental values are made for the parameters of the recently studied $GaAs/Al_{0.3}Ga_{0.7}As$ SL.[19] Let us emphasize that the focus of our approach is to elucidate the basic physics of the localized resonant exciton states in biased SL. We do not intend to compete with the results obtained by comprehensive numerical methods.

The paper is organized as follows: In Secs. II and III, the quasienergetic exciton states and the coefficient of multiphoton exciton absorption are calculated, respectively, in the approximation of a single WSL. The exciton absorption related to the resonant exciton states is studied in the double-WSL approximation in Sec. IV. A discussion of the obtained results, justification of the employed simplifications, as well as a comparison with the available experimental data and estimates of the expected experimental values are provided in Sec. V. Section VI contains the conclusions.

II. QUASIENERGETIC EXCITON STATES

We consider multiphoton absorption in a semiconductor SL associated with the transition of a crystal from an initial state to an excited exciton state in the presence of a uniform electric field $\mathbf{E}$. We have an oscillating electric field $\mathbf{F}_0 \cos \omega t$ of frequency ω and magnitude F_0 and a dc field $\mathbf{E}$ both directed parallel to the z axis. The latter is perpendicular to the heteroplanes. Mott exciton is formed by the Coulomb interaction between the electron (e) in the conduction band and the hole (h) in the valence band, both taken to be parabolic, nondegenerate, and separated by a wide energy gap $\mathcal{E}_g$.

In the effective-mass approximation and using the cylindrical coordinates $\boldsymbol{\rho}$ and z, the wave function Ψ of the exciton formed by the particles having the effective masses m_j, charges e_j ($e_e = -e_h = -e$), and positions $\mathbf{r}_j(\boldsymbol{\rho}_j, z_j)$, $j = e, h$, obeys the equation

$$\left\{ \sum_{j=e,h} \left[-\frac{\hbar^2}{2m_j} \Delta_j + V_j(z_j) + e_j F(t) z_j \right] - \frac{e^2}{4\pi\varepsilon_0 \kappa \sqrt{(\boldsymbol{\rho}_e - \boldsymbol{\rho}_h)^2 + (z_e - z_h)^2}} - i\hbar \frac{\partial}{\partial t} \right\} \Psi(\mathbf{r}_e, \mathbf{r}_h, t) = \mathbf{0}, \tag{1}$$

where $F(t) = E + F_0 \cos \omega t$, κ is the dielectric constant, and V_j is the SL potential consisting of the periodic sequence of the large number N of the quantum wells of width d separated by the potential barriers. Further, we assume that the Coulomb interaction between the electron and hole does not effect strongly the longitudinal states governed by the SL potentials $V_j(z_j)$ and electric field $F(t)$. This assumption implies that the distance between the minibands $\hbar^2/2m_j d^2$ associated with the potentials $V_j(z_j)$ and that between the WSLs eEd both considerably exceed the exciton Rydberg constant,

$$\mathrm{Ry} = \frac{\hbar^2}{2m_{ex} a_0^2}, \quad m_{ex}^{-1} = m_e^{-1} + m_h^{-1}, \quad a_0 = \frac{4\pi\varepsilon_0 \varepsilon \hbar^2}{m_{ex} e^2},$$

a_0 being the excition Bohr radius.

The mentioned conditions $d \ll a_0$ and $\mathrm{Ry} \ll eEd$ allow us to consider the carriers to be related to the ground electron and hole minibands and single electron-hole WSL. In this single-WSL approximation, the exciton wave function Ψ can be written in the form

$$\Psi_{\nu\mu}(\mathbf{r}_e,\mathbf{r}_h,t) = \frac{1}{\sqrt{L_xL_y}}\exp\left[i\left(\mathbf{K}_\perp\mathbf{R}_\perp - \frac{\mathcal{E}}{\hbar}t\right)\right] f_{e\nu}(z_e,t) f_{h\mu}(z_h,t)\Phi_{\nu\mu}(\boldsymbol{\rho},t), \tag{2}$$

where

$$\boldsymbol{\rho} = \boldsymbol{\rho}_e - \boldsymbol{\rho}_h \quad \text{and} \quad \mathbf{R}_\perp = \frac{m_e\boldsymbol{\rho}_e + m_h\boldsymbol{\rho}_h}{m_e + m_h}$$

are a transverse relative coordinate and a coordinate of the center of mass, respectively. $\hbar\mathbf{K}_\perp$ is the transverse total momentum of the exciton, L_x, L_y are the transverse linear dimensions of the crystal, $\mathcal{E}$ is the quasienergy of the exciton, and $f_j(z_j,t)=f_j(z_j,t+T)$ and $\Phi(\boldsymbol{\rho},t)=\Phi(\boldsymbol{\rho},t+T)$ $(T=2\pi/\omega)$ are the periodic wave functions of the longitudinal and transverse quasienergetic states, respectively. The longitudinal functions $f_j(z_j,t)$ satisfy the equation

$$\left[-\frac{\hbar^2}{2m_j}\frac{\partial^2}{\partial z_j^2} + V_j(z_j) + e_jF(t)z_j - \mathcal{E}_j - i\hbar\frac{\partial}{\partial t}\right] f_j(z_j,t) = 0,$$

$$j = e,h, \tag{3}$$

where $\mathcal{E}_j$ are the quasienergies of the carriers.

In an effort to develop an analytical approach to the problem, we simulate the SL potentials $V_j(z_j)$ by a chain of period d of δ-function-type barriers of the powers β_j,

$$V_j(z_j) = \beta_j\sum_{s=0}^{N}\delta(z_j - sd), \quad V_j(z_j) = V_j(z_j + d). \tag{4}$$

This model devised originally in Ref. 34 has been applied successfully to the problems of one-photon electro- and 2D exciton absorption,[34] multiphoton 2D exciton absorption in the absence of dc electric fields,[35] and multiphoton electro-[36] and magnetoelectroabsorption,[37] thereby ignoring exciton effects.

The solution to Eq. (3) with the potentials $V_j(z_j)$ [Eq. (4)] at $F(t)=0$, determining the energies of the ground minibands $\mathcal{E}_j \equiv \varepsilon_j(k_j)=\varepsilon_j(k_j+2\pi/d)$ and the SL Bloch functions $f_j(z_j,t)\equiv\psi_j(z_j,k_j)=\psi_j(z_j,k_j+2\pi/d)$, can be found in explicit form,[34]

$$\varepsilon_j(k_j) \equiv \varepsilon_j(\alpha_j) = b_j + \Delta_j\sin^2\frac{\alpha_j}{2}, \quad b_j = \frac{\hbar^2\pi^2}{2m_jd^2}(1 - 8\lambda_j),$$

$$\Delta_j = \frac{\hbar^2\pi^2}{2m_jd^2}8\lambda_j, \quad \lambda_j = \frac{\hbar^2}{2m_jd\beta_j} \ll 1, \tag{5}$$

$$\psi_j(z_j,k_j) \equiv \psi_j(z_j,\alpha_j) = \frac{i}{\sqrt{N}}e^{is\alpha_j}u_s(z_j)[1 + O(\lambda_j)],$$

$$\alpha_j = k_jd, \quad \langle\psi(z,k)|\psi(z,k')\rangle = \delta_{kk'}, \tag{6}$$

where within the sth cell

$$u_s(z) = \sqrt{\frac{2}{d}}\sin\frac{\pi}{d}(z - sd), \quad ds \leqslant z \leqslant d(s+1).$$

The energies b_j and Δ_j represent the bottom and width of the ground minibands, respectively. λ_j are treated as parameters of the theory, but they can be calculated knowing the characteristics of the SL.[34] Clearly, our approach is valid in the nearest-neighbor tight-binding approximation $(\lambda_j \ll 1)$.[13] In this approximation, the dispersion law $\varepsilon_j(k_j)$ has form (5) and the wave function ψ is the sum of phase-shifted wave functions $u_s(z)$ describing the carrier in an isolated quantum well bounded by infinite potential barrier $(\beta_j=\infty, \lambda_j=0)$. In the wave functions (6), the correction terms of the order of $\lambda_j u_s$ take into account the finite penetrability of the barriers $(\beta_j \neq \infty, \lambda_j \ll 1)$. In particular, the interwell coupling leads to the result that the Wannier functions corresponding to the Bloch functions ψ [Eq. (6)] become localized not only within the sth cell $(\sim u_s)$ but also in the neighboring $s\pm1$ cells $(\sim\lambda_j u_s)$. Explicit expressions for the correction terms and for the Wannier functions can be found in Ref. 34. In order to remain in the framework of the nearest-neighbor tight-binding approximation in the presence of the dc electric field E, we assume that the total potential drop on the length of the SL is larger than the miniband width $\Delta_j (NeEd \gg \Delta_j)$ (see Ref. 1 in Ref. 13).

For the short-period SLs typically used in experiments and even for sufficiently strong dc electric fields E, the condition $eEd \ll \hbar\omega$ remains valid. For example, if $\hbar\omega \sim 1$ eV, $d \sim 60$ Å, and $E \sim 100$ kV/cm, then the ratio $eEd/\hbar\omega$ is about 0.06. As is shown in Ref. 36, under this condition the electron function $f_e(z_e,t)$ obeying Eq. (3) for $F(t)\neq 0$ can be written in the form

$$f_{e\nu}(z_e,t) = \frac{\sqrt{N}}{2\pi}\int_{-\pi}^{+\pi}\psi_e[q_e(\alpha_e,\phi),z_e]c_{e\nu}(\alpha_e,\phi)d\alpha_e, \quad \phi = \omega t, \tag{7}$$

where

$$c_{e\nu}(\alpha_e,\phi) = \exp\left\{-\frac{i}{\hbar\omega}\int_0^\phi[\varepsilon_e(\alpha_e,\vartheta) - \bar{\varepsilon}_e(\alpha_e)]d\vartheta - \frac{i}{eEd}\int_0^{\alpha_e}\left[\bar{\varepsilon}_e(\theta) - \mathcal{E}_{e\nu} + \frac{1}{2}eEd\right]d\theta\right\}, \tag{8}$$

$$\bar{\varepsilon}_e(\alpha_e) = \frac{1}{2\pi}\int_0^{2\pi}\varepsilon_e(\alpha_e,\phi)d\phi, \quad \varepsilon_e(\alpha_e,\phi) \equiv \varepsilon_e(q_e),$$

$$q_e(\alpha_e,\phi) = \alpha_e + \gamma\sin\phi, \quad \gamma = \frac{eF_0d}{\hbar\omega},$$

$$c_{e\nu}(\alpha,\phi) = c_{e\nu}(\alpha + 2\pi,\phi) = c_{e\nu}(\alpha,\phi + 2\pi),$$

$$\langle f_{e\nu}(z_e,t)|f_{e\nu'}(z_e,t)\rangle = \delta_{\nu\nu'},$$

and

$$\mathcal{E}_{e\nu} = b_e + \frac{1}{2}\Delta_e + eEd\left(\nu + \frac{1}{2}\right), \quad \nu = 0, \pm1, \pm2, \ldots \tag{9}$$

are the WSLs, counted from the bottom of the conduction band.

Using Eq. (5) for $\varepsilon_e(q_e)$, we obtain from Eq. (8) for the electron function in explicit form

$$c_{e\nu}(\alpha_e,\phi) = \exp\left\{ i\xi_e[\sin\alpha_e\Phi_1(\phi) + \cos\alpha_e\Phi_2(\phi)] - \frac{i}{2}\gamma\sin\phi \right\} \times \exp[i(\zeta_e\sin\alpha_e + \nu\alpha_e)], \quad (10)$$

with

$$\Phi_1(\phi) = -\sum_{n=1}^{\infty}\frac{J_{2n-1}(\gamma)}{2n-1}[1-\cos(2n-1)\phi],$$

$$\Phi_2(\phi) = \sum_{n=1}^{\infty}\frac{J_{2n}(\gamma)}{2n}\sin 2n\phi, \quad \xi_e = \frac{\Delta_e}{\hbar\omega}, \quad \zeta_e = \frac{\Delta_e}{2eEd}J_0(\gamma).$$

$J_n(\gamma)$ are the Bessel functions. At this stage, we take into account that in realistic SLs the widths of the minibands Δ_j are much less than the energy gap $\mathcal{E}_g \sim \hbar\omega$, yielding $\Delta_j \ll \hbar\omega$. For $\Delta_j \sim 0.05$ eV and $\hbar\omega \sim 1$ eV, we have $\xi_j = \Delta_j/\hbar\omega \sim 0.05$. On expanding the functions $c_{e\nu}(\alpha_e,\phi)$ [Eq. (10)] in the power series with respect to the parameter ξ_e, we obtain from Eq. (7) for the sth cell

$$f_{e\nu}(z_e,t) = e^{i(s-1/2)\gamma\sin\phi}u_s(z_e)\left(J_{-(\nu+s)}(\zeta_e) + \frac{\xi_e}{2}\{[\Phi_1(\phi)+i\Phi_2(\phi)]J_{-(\nu+s+1)}(\zeta_e) + [-\Phi_1(\phi)+i\Phi_2(\phi)]J_{-(\nu+s-1)}(\zeta_e)\}\right). \quad (11)$$

In the limiting case $\zeta_e \ll 1$, the Bessel functions in Eq. (11) transform into $J_{-(n+s)} \simeq \delta_{s,-n}$, which in turn means that the wave function $f_{e\nu}(z_e,t)$ [Eq. (11)] of the electron having the energy $\mathcal{E}_{e\nu}$ [Eq. (9)] becomes completely localized within the $s=-\nu$ cell (time-independent part) and within the $s=-\nu\pm1$ cells [time-dependent part $\sim\frac{1}{2}\xi_e\Phi_{1,2}(\phi)$]. The hole function $f_{h\mu}(z_h,t)$ and the hole WSL $\mathcal{E}_{h\mu}$ can be obtained from the electron function $f_{e\nu}(z_e,t)$ [Eq. (11)] and from the electron WSL $\mathcal{E}_{e\nu}$ [Eq. (9)] by replacing in Eqs. (9) and (11) the electric charge e by $-e$, index e by index h, t by $-t$, and ν by μ and finally taking the complex conjugate. The hole WSLs obtained from Eq. (9) are to be counted from the top of the valence band.

In sufficiently strong dc electric fields, the distance between the neighboring WSLs eEd becomes much greater than the Coulomb energy of the exciton, i.e., $eEd \gg$ Ry. This allows us to consider the quasi-2D exciton states as being associated with the isolated electron-hole WSL $\mathcal{E}_{\nu\mu} = \mathcal{E}_{e\nu} + \mathcal{E}_{h\mu}$ (single-WSL approximation), where

$$\mathcal{E}_{\nu\mu} \equiv \mathcal{E}_\sigma = \mathcal{E}_g + b_e + b_h + 1/2(\Delta_e + \Delta_h) + eEd\sigma, \quad (12)$$

$$\sigma = \nu - \mu = 0, \pm 1, \pm 2, \ldots .$$

In this case, we have for the function $\Phi_{\nu\mu}(\boldsymbol{\rho},t)$ from Eqs. (1)–(3)

$$\left[-\frac{\hbar^2}{2m_{ex}}\Delta + U_{\nu\mu}(\rho,t) + \left(\mathcal{E}_\sigma + \frac{\hbar^2K_\perp^2}{2M} - \mathcal{E} \right) - i\hbar\frac{\partial}{\partial t} \right]\Phi_{\nu\mu}(\boldsymbol{\rho},t) = 0, \quad (13)$$

with

$$U_{\nu\mu}(\rho,t) = -\frac{e^2}{4\pi\varepsilon_0\kappa}\int_0^{Nd}\frac{|f_{e\nu}(z_e,t)|^2|f_{h\mu}(z_h,t)|^2}{\sqrt{\rho^2+(z_e-z_h)^2}}dz_e dz_h, \quad (14)$$

where the functions $f_j(z_j,t)$ are determined by Eq. (11).

Further, we concentrate on the most attractive case of the sufficiently strong dc electric field satisfying the condition $\zeta_j \simeq (\Delta_j/2eEd) \leqslant 1$ that, in turn, provides the localization of the carriers within one period of the SL. For a GaAs/AlGaAs SL consisting of QWs of width $d=65$ Å ($\Delta_j \sim 0.07$ meV),[18] electric fields of strength $E \geqslant 55$ kV/cm are required.

Under the condition $\zeta_j < 1$, the electron (hole) charge density described by the functions (11) mostly concentrates within the cell $s=-\nu$ ($s'=-\mu$). For $\zeta_e=0.6$, the contribution to the neighboring cells $s=\nu\pm1$ is of the order of 0.07. As a result, the potential $U_{\nu\mu}(\rho,t)$ calculated by using the functions (11) under the conditions $\xi_j \ll 1$ and $\zeta_j < 1$ can be written in the form

$$U_{\nu\mu}(\rho,t) \equiv U_\sigma(\rho) = -\frac{D_{eh}e^2}{4\pi\varepsilon_0\kappa}\left\langle 0\left|\frac{1}{\sqrt{\rho^2+(z_e-z_h-\sigma d)^2}}\right|0\right\rangle \times[1+O(\xi_j\Phi_{1,2}(\phi))], \quad \sigma = 0, \pm1, \pm2, \ldots . \quad (15)$$

$\langle 0|\ldots|0\rangle$ is an average with respect to the function $u_0(z_e)u_0(z_h)$ determined in Eq. (6) and

$$D_{eh}(E) = J_0^2(\zeta_e)J_0^2(\zeta_h) \quad \text{with} \quad D_{eh} = 1 - \frac{1}{4}(\zeta_e^2+\zeta_h^2) \quad \text{at} \quad \zeta_{eh} \ll 1. \quad (16)$$

The coefficient D_{eh} [Eq. (16)] accounts for the extent to which the carriers are localized within one cell of the SL.

Since the optical dipole transitions are allowed to the cylindrically symmetric states with the magnetic quantum number $m=0$ and for the total momentum $\hbar\mathbf{K}_\perp \simeq 0$,[41] the function $\Phi_{\nu\mu}(\boldsymbol{\rho},t) \equiv \Phi_\sigma(\rho) = \frac{1}{\sqrt{2\pi}}R_\sigma(\rho)$ in Eq. (13) satisfies

$$\left[-\frac{\hbar^2}{2m_{ex}}\frac{1}{\rho}\frac{d}{d\rho}\left(\rho\frac{d}{d\rho}\right) + U_\sigma(\rho) + \frac{4\overline{\mathrm{Ry}}}{n^2} \right]R_\sigma(\rho) = 0,$$

$$\mathcal{E} = \mathcal{E}_\sigma - \frac{4\overline{\mathrm{Ry}}}{n^2}, \quad \overline{\mathrm{Ry}} = D_{eh}^2\mathrm{Ry}. \quad (17)$$

In the following, we provide a brief outline of our method to solve Eq. (17). Further details can be found in Ref. 38 where this approach was developed originally.

For $\rho \gg d$, the solution to Eq. (17) becomes

$$R_\sigma(\rho) = A_\sigma u^{-1/2} W_{n/2,0}(u), \quad u = \frac{4\rho}{n\bar{a}_0}, \quad \bar{a}_0 = \frac{a_0}{D_{eh}}, \quad (18)$$

where $W_{n/2,0}(u)$ is the Whittaker function[39] and where A_σ is a constant. In the region $\rho \ll \bar{a}_0$ $(u \ll 1)$, an iteration procedure is performed by double integration of Eq. (17) using the trial function $R^0_\sigma(\rho, z_e - z_h)$,

$$R^{(0)}_\sigma(\rho, z_e - z_h) = c_\sigma \left[\ln\left(u + \sqrt{u^2 + \frac{g_\sigma^2}{n^2}} \right) + \alpha_\sigma \right],$$

$$g_\sigma(z_e, z_h) = \frac{4|z_e - z_h - \sigma d|}{\bar{a}_0} \ll 1, \quad (19)$$

and its derivative $R^{0\prime}_\sigma(\rho, z_e - z_h)$,

$$R^{(0)\prime}_\sigma(\rho, z_e - z_h) = c_\sigma \left[\frac{1}{\sqrt{u^2 + \frac{g_\sigma^2}{n^2}}} - \frac{n}{g_\sigma} - \frac{n}{2} \frac{u}{\sqrt{u^2 + \frac{g_\sigma^2}{n^2}}} \times \ln\left(u + \sqrt{u^2 + \frac{g_\sigma^2}{n^2}} \right) \right], \quad (20)$$

where α_σ and c_σ are constants. We imply that in Eq. (17), the 2D potential $U(\rho)$ [Eq. (15)] is replaced by the three-dimensional Coulomb potential used in Eq. (1). The averaging with respect to the coordinates z_e, z_h is performed at the final stage of the iteration procedure. As a result, we have

$$R_\sigma(\rho) = c_\sigma \left[\ln u + \alpha_\sigma + n\left(\frac{1}{\bar{g}_\sigma} - \frac{\alpha_\sigma}{2} \right) u \ln u \right], \quad (21)$$

with $\bar{g}_\sigma = \langle 0 | g_\sigma(z_e, z_h) | 0 \rangle$. In the region $\rho \ll \bar{a}_0$ $(u \ll 1)$, the function $R_\sigma(\rho)$ [Eq. (18)] transforms into[39]

$$R_\sigma(\rho) = -\frac{A_\sigma}{\Gamma\left(\frac{1-n}{2}\right)} \left[\ln u + \psi\left(\frac{1-n}{2}\right) + 2C - \frac{n}{2} u \ln u \right], \quad (22)$$

where $\psi(x)$ is the psi function [the logarithmic derivative of the gamma function $\Gamma(x)$] and $C = 0.577$ is the Euler constant. When terms of the same order in Eqs. (21) and (22) are equated, we obtain $n = n_0 + \bar{g}_\sigma$, $n_0 = 1, 3, 5, \ldots$, and

$$\bar{g}_0 = \frac{4}{3}\left(1 - \frac{15}{4\pi^2}\right)\frac{d}{\bar{a}_0}, \quad \bar{g}_{\pm 1} = \frac{16}{3}\left(1 - \frac{15}{16\pi^2}\right)\frac{d}{\bar{a}_0}. \quad (23)$$

In this approximation, the solutions to Eq. (17) $R_{\sigma n}(\rho)$ are the 2D wave functions of the discrete Coulomb energy spectrum with[40]

$$|\Phi_{\sigma n}(0)|^2 = \frac{8}{\pi \bar{a}_0^2 (n_0 + \bar{g}_\sigma)^3}, \quad n_0 = 1, 3, \ldots. \quad (24)$$

Note that the correction to the energy of the ideal 2D exciton $(n = n_0)$ induced by the chosen trial function (19) and trial derivative (20) $(n = n_0 + \bar{g}_\sigma)$ coincides exactly with that calculated by perturbation theory. The continuous energies $\mathcal{E} - \mathcal{E}_\sigma = \frac{\hbar^2 k_\perp^2}{2m_{ex}} > 0$ in Eq. (13) with $K_\perp = 0$ correspond to unbound quasi-2D exciton states with[34]

$$|\Phi_{\sigma k_\perp}(0)|^2 = \frac{\exp\left(\frac{\pi}{k_\perp \bar{a}_0}\right)}{4\pi^2 \cosh\left(\frac{\pi}{k_\perp \bar{a}_0}\right)}. \quad (25)$$

Thus, in the single-WSL approximation the energy spectrum of the spatially localized exciton is a sequence of quasi-Rydberg series of discrete levels $n_0 = 1, 3, 5, \ldots$, each adjacent from the low-energy side to the WSL $\mathcal{E}_\sigma$ [Eq. (12)] and covered by the branches of the continuous $(k_\perp)$ spectrum emanating from the WSLs $\sigma - 1, \sigma - 2, \ldots$.

III. MULTIPHOTON EXCITON ABSORPTION IN THE SINGLE-WSL APPROXIMATION

We treat the optical absorption as a transition of the electron-hole pair from the initial state to an excited state described by the wave functions $\Psi_0(\mathbf{r}_e, \mathbf{r}_h) = \delta(\mathbf{r}_e - \mathbf{r}_h)$ (Ref. 41) and $\Psi(\mathbf{r}_e, \mathbf{r}_h, t)$ [Eq. (2)], respectively. The coefficient α of the light absorption with the oscillating electric field $F_0 \cos \omega t$ in the crystal of volume $\Omega = L_x L_y N d$ possessing the refractive index $\bar{n}$ is determined by the transition rate

$$W = \frac{1}{t} \sum_{e,h} |S(t)|^2, \quad \alpha = \frac{\bar{n}\hbar\omega}{c v \Omega} W, \quad (26)$$

where c is the speed of light, $v = \varepsilon_0 \bar{n}^2 F_0^2$ is the optical energy density, $\Sigma_{e,h}$ is a sum over the exciton states, and $S(t)$ is the matrix element of the operator of the dipole transition $P(t) = P_0 \cos \omega t$,

$$S(t) = \frac{1}{i\hbar} \int_0^t \delta(\mathbf{r}_e - \mathbf{r}_h) P(\tau) \Psi^*(\mathbf{r}_e, \mathbf{r}_h, \tau) d\mathbf{r}_e d\mathbf{r}_h d\tau,$$

$$P_0 = \frac{i\hbar e F_0 p_{ehz}}{m_0 \mathcal{E}_g}. \quad (27)$$

In Eq. (26), p_{ehz} is the matrix element of the momentum operator calculated with respect to the Bloch amplitudes of the electron and hole bands. On substituting Ψ from Eq. (2) into Eq. (27), we obtain

$$S(t) = \frac{P_0}{i\hbar} \int_0^t \exp\left(\frac{i}{\hbar}\mathcal{E}\tau\right) M(\tau) \cos \omega\tau d\tau, \quad (28)$$

with

$$M(\tau) = \sqrt{L_x L_y} \Phi^*_{\sigma n(k_\perp)}(0) \int_0^{Nd} f^*_{ev}(z, \tau) f^*_{h\mu}(z, \tau) dz,$$

$$M(t + T) = M(t). \quad (29)$$

Using the expansion

$$M(\tau)\cos\omega\tau = \sum_{l=-\infty}^{+\infty} e^{-il\omega\tau} A_l(\omega),$$

$$A_l(\omega) = \frac{\omega}{2\pi}\int_{-\pi/\omega}^{+\pi/\omega} e^{il\omega t}\cos\omega t M(t)dt, \tag{30}$$

α can be written as a sum of the coefficients of l-photon absorption α_l,

$$\alpha = \sum_l \alpha_l, \quad \alpha_l(\omega) = \frac{\bar{n}\hbar\omega}{cv\Omega} P_0^2 \frac{2\pi}{\hbar}\sum_{e,h} |A_l(\omega)|^2 \delta(\mathcal{E} - l\hbar\omega),$$

$$l = 1,2,3,\ldots. \tag{31}$$

The exciton energy $\mathcal{E}$ is given by

$$\mathcal{E} \equiv \mathcal{E}_{\sigma n_0(k_\perp)} = \mathcal{E}_\sigma + \begin{cases} -\dfrac{4\overline{\mathrm{Ry}}}{(n_0+\bar{g}_\sigma)^2}, & \text{discrete states} \\ \dfrac{\hbar^2 k_\perp^2}{2m_{ex}}, & \text{continuous states,} \end{cases} \tag{32}$$

$$\sum_{e,h} \equiv N\sum_\sigma \times \begin{cases} \sum_{n_0} \\ \int d\vec{k}_\perp. \end{cases}$$

Substituting the functions $f_{j\nu(\mu)}(z,t)$ [Eq. (11)] into Eq. (29), we obtain for the coefficient of the l-photon absorption $\alpha_l(\omega)$

$$\alpha_l(\omega) = \alpha_0 \sum_\sigma C_\sigma^{(l)}(\gamma,\zeta) G_\sigma^{(l)}(\omega), \tag{33}$$

with

$$C_\sigma^{(l)}(\gamma,\zeta) = \{\delta_{l1} J_{-\sigma}(\zeta) + (1-\delta_{l1})\xi Q_l(\gamma) \times [J_{-\sigma-1}(\zeta) \pm J_{-\sigma+1}(\zeta)]\}^2. \tag{34}$$

The sign + (−) corresponds to an odd (even) number of photons l. We have

$$G_\sigma^{(l)}(\omega) = \sum_{n_0(\vec{k}_\perp)} |\Phi_{\sigma n(k_\perp)}(0)|^2 \delta(l\hbar\omega - \mathcal{E}_{\sigma n_0(k_\perp)}). \tag{35}$$

In Eqs. (33)–(35), the following notations are employed:

$$\zeta = \zeta_e + \zeta_h, \quad \xi = \xi_e + \xi_h,$$

$$Q_l(\gamma) = \frac{1}{4}\left[\frac{J_{l+1}(\gamma)}{l+1} + \frac{J_{l-1}(\gamma)}{l-1}\right],$$

$$\alpha_0 = \frac{\pi\omega\hbar^2 e^2 |p_{ehz}|^2}{2\varepsilon_0 \bar{n} c d m_0^2 \mathcal{E}_g^2}.$$

It follows from Eq. (34) that in the case of a sufficiently strong dc electric field providing the localization ($\zeta < 1$), the terms $\sigma = 0, \pm 1$ contribute mostly to $\alpha_l(\omega)$ [Eq. (33)]. Taking Eqs. (24) and (25) for $|\Phi_{\sigma n(k_\perp)}(0)|^2$ in Eq. (35), we obtain for the coefficient of l-photon absorption $\alpha_l(\omega)$

(a) discrete optical spectrum,

$$\begin{aligned}\alpha_l(\omega) = \alpha_0 \sum_{n_0=1} \frac{8}{\pi \bar{a}_0^2}[&\delta_{l1}((n_0+\bar{g}_0)^{-3} J_0^2(\zeta)\delta[l\hbar\omega - \mathcal{E}_0^{(0)}(n_0)] \\ &+ (n_0+\bar{g}_{\pm1})^{-3} J_1^2(\zeta)\{\delta[l\hbar\omega - \mathcal{E}_{-1}^{(0)}(n_0)] \\ &+ \delta[l\hbar\omega - \mathcal{E}_{+1}^{(0)}(n_0)]\}) + (1-\delta_{l1})\xi^2 Q_l(\gamma)^2((n_0 \\ &+ \bar{g}_0)^{-3}[J_1(\zeta) \pm J_{-1}(\zeta)]^2 \delta[l\hbar\omega - \mathcal{E}_0^{(0)}(n_0)] \\ &+ (n_0+\bar{g}_{\pm1})^{-3}[J_0(\zeta) \pm J_2(\zeta)]^2\{\delta[l\hbar\omega - \mathcal{E}_{-1}^{(0)}(n_0)] \\ &+ \delta[l\hbar\omega - \mathcal{E}_{+1}^{(0)}(n_0)]\})],\end{aligned} \tag{36}$$

(b) continuous optical spectrum,

$$\begin{aligned}\alpha_l(\omega) = \alpha_0 \frac{m_{ex}}{2\pi\hbar^2}\Bigg\{&\delta_{l1}\Bigg[J_0^2(\zeta)\frac{\exp[\beta_0^{(l)}(\omega)]}{\cosh[\beta_0^{(l)}(\omega)]} \\ &+ J_1^2(\zeta)\left(\frac{\exp[\beta_{-1}(l)(\omega)]}{\cosh[\beta_{-1}^{(l)}(\omega)]} + \frac{\exp[\beta_{+1}(l)(\omega)]}{\cosh[\beta_{+1}^{(l)}(\omega)]}\right)\Bigg] \\ &+ (1-\delta_{l1})\xi^2 Q_l(\gamma)^2\Bigg[[J_1(\zeta) \pm J_{-1}(\zeta)]^2 \frac{\exp[\beta_0^{(l)}(\omega)]}{\cosh[\beta_0^{(l)}(\omega)]} \\ &+ (J_0(\zeta) \pm J_2(\zeta))^2\Bigg(\frac{\exp[\beta_{-1}(l)(\omega)]}{\cosh[\beta_{-1}^{(l)}(\omega)]} \\ &+ \frac{\exp[\beta_{+1}(l)(\omega)]}{\cosh[\beta_{+1}^{(l)}(\omega)]}\Bigg)\Bigg]\Bigg\}.\end{aligned} \tag{37}$$

Here, we have used

$$\mathcal{E}_\sigma^{(0)}(n_0) = \mathcal{E}_\sigma - \frac{4\overline{\mathrm{Ry}}}{(n_0+\bar{g}_\sigma)^2}, \quad n_0 = 1,3,\ldots, \tag{38}$$

$$\beta_\sigma^{(l)}(\omega) = \frac{\pi}{\bar{a}_0\sqrt{\frac{2m_{ex}}{\hbar^2}(l\hbar\omega - \mathcal{E}_\sigma)}}. \tag{39}$$

The energies $\mathcal{E}_\sigma^{(0)}(n_0)$ [Eq. (38)] determine the exciton δ-function-type peak positions in the single-WSL approximation, while the Bessel functions $J_k(\zeta)$ ($k = 0, \pm 1, 2$) govern the effect of the dc electric field on the intensities of the exciton maxima. With increasing the electric field E, Eqs. (36) and (37) are simplified by taking $J_0(\zeta) \simeq 1$, $J_{\pm1}(\zeta) \simeq \pm\frac{\zeta}{2}$, $J_2(\zeta) \simeq \frac{\zeta^2}{8}$ at $\zeta \ll 1$. In the absence of the exciton formation, the expression for the coefficient of the l-photon absorption α_l can be obtained from Eq. (37) by replacing $\frac{\exp[\beta_\sigma^{(l)}(\omega)]}{\cosh[\beta_\sigma^{(l)}(\omega)]}$ by the unit step function $\Theta(l\hbar\omega - \mathcal{E}_\sigma)$, $\sigma = 0, \pm 1$. In this case, our results [Eq. (37)] transform into those obtained earlier in Refs. 34 and 36 in which one-photon and multiphoton electroabsorption in SL have been considered, respectively.

IV. MULTIPHOTON EXCITON ABSORPTION IN DOUBLE-WSL APPROXIMATION

In the single-WSL approximation considered above, the exciton energy $\mathcal{E}$ in Eq. (32) consists of a sequence of series of quasi-Coulomb levels $\simeq \frac{-4\overline{Ry}}{n_0^2}$ adjacent on the low-energy side to the WSL $\mathcal{E}_\sigma$ [Eq. (12)]. The density of the exciton states is a sum of δ-function-type singularities reflected in the absorption coefficient (36). The strictly discrete character of the exciton states is the result of the single-WSL approximation ignoring the resonant coupling between the quasi-Coulomb levels adjacent to the WSL $\mathcal{E}_\sigma$ and branches of the continuous spectra $\frac{\hbar^2 k_\perp^2}{2m_{ex}}$ emanating from the WSLs $\sigma-1, \sigma-2, \sigma-3, \ldots$. In fact, the resonant coupling leads to an autoionization of the exciton states. The autoionization rate $\Gamma_\sigma(n_0)/\hbar$ and lifetime $\tau_\sigma(n_0)=\hbar/\Gamma_\sigma(n_0)$ both are related to the width $\Gamma_\sigma(n_0)$ of the n_0 exciton state, associated with the σ WSL.

Below, we consider a double-WSL approximation describing the interaction between the quasi-Coulomb states $n_0=1,3,5,\ldots$ adjacent to the WSL $\mathcal{E}_\sigma$ and the states of the continuous spectrum, emanating from the WSL $\mathcal{E}_{\sigma-1}$. The spectrum of the exciton absorption has been calculated by two methods. In the first approach, the real wave function corresponding to the real energy of the continuous state is taken in the form of a standing wave. We have found the complete profile of the exciton absorption that transforms in the vicinity of the peak position into a Lorentzian form determined by the resonant width and shift. Exactly the same width and shift have been found in the second approach for which the wave function of the continuous state is taken in the form of an outgoing-type wave. The real and imaginary parts of the complex exciton energies determine the positions and widths of the exciton peaks, respectively. Since in this paper we focus on the narrow region close to the peak position, we follow the considerably less cumbersome second method. Also, we provide a brief description of the first approach. Both methods have been originally developed in Ref. 38 and successfully applied to the resonant impurity and exciton states in a single QW.

Since the optical dipole transitions are allowed in the cylindrically symmetric exciton states with the transverse total momentum $\hbar\mathbf{K}_\perp \simeq 0$, the quasienergetic solution to Eq. (1) Ψ corresponding to the quasienergy $\mathcal{E}$ can be written in the form

$$\Psi(\rho,z_e,z_h,t) = \frac{1}{\sqrt{L_x L_y}}\frac{1}{\sqrt{2\pi}}\exp\left(-\frac{i}{\hbar}\mathcal{E}t\right) \times \sum_{\nu'\mu'} f_{e\nu'}(z_e,t) f_{h\mu'}(z_h,t) R_{\nu'\mu'}(\rho,t), \quad (40)$$

where $f_j(z_j,t)$ are the electron $j=e$ and hole $j=h$ periodic longitudinal wave functions [Eq. (11)], satisfying Eq. (3), and where $R_{\nu\mu}(\rho,t+T)=R_{\nu\mu}(\rho,t)$ are the periodic transverse wave functions. Substituting Ψ of Eq. (40) into Eq. (1), we arrive at a set of equations for the radial functions $R_{\nu\mu}(\rho,t)$,

$$\left[-\frac{\hbar^2}{2m_{ex}}\left(\frac{1}{\rho}\frac{d}{d\rho}\rho\frac{d}{d\rho}\right) + (\mathcal{E}_\sigma - \mathcal{E}) - i\hbar\frac{\partial}{\partial t}\right] R_{\nu\mu}(\rho,t) + \sum_{\nu'\mu'} U_{\nu\mu}^{\nu'\mu'}(\rho,t) R_{\nu'\mu'}(\rho,t) = 0, \quad (41)$$

with

$$U_{\nu\mu}^{\nu'\mu'}(\rho,t) = -\frac{e^2}{4\pi\varepsilon_0\kappa}\int_0^{Nd} dz_e dz_h \times \frac{f_{e\nu'}(z_e,t) f_{h\mu'}(z_h,t) f_{e\nu}^*(z_e,t) f_{h\mu}^*(z_h,t)}{\sqrt{\rho^2+(z_e-z_h)^2}}. \quad (42)$$

The WSLs $\mathcal{E}_\sigma$ are given by Eq. (12). Below, we consider the coupling between the localized ($\zeta_j<1$) discrete $n_0=1,3,\ldots$ states adjacent to the WSL $\mathcal{E}_0$ and continuous $k_\perp$ states branching from the WSL $\mathcal{E}_{-1}$. Exciton series relevant to $\sigma=0$ is the most intense in the spectrum of the one-photon absorption. The set of equations (41) with the potentials (42) calculated with the help of the functions (11) becomes

$$\left[-\frac{\hbar^2}{2m_{ex}}\left(\frac{1}{\rho}\frac{d}{d\rho}\rho\frac{d}{d\rho}\right) + U_0(\rho) + (\mathcal{E}_0 - \mathcal{E})\right] R_0(\rho) + \left[\frac{J_1(\zeta_e)}{J_0(\zeta_e)} + \frac{J_1(\zeta_h)}{J_0(\zeta_h)}\right][U_0(\rho) - U_{-1}(\rho)] R_{-1}(\rho) = 0, \quad (43)$$

$$\left[-\frac{\hbar^2}{2m_{ex}}\left(\frac{1}{\rho}\frac{d}{d\rho}\rho\frac{d}{d\rho}\right) + U_{-1}(\rho) + (\mathcal{E}_{-1} - \mathcal{E})\right] R_{-1}(\rho) + \left[\frac{J_1(\zeta_e)}{J_0(\zeta_e)} + \frac{J_1(\zeta_h)}{J_0(\zeta_h)}\right][U_0(\rho) - U_{-1}(\rho)] R_0(\rho) = 0. \quad (44)$$

The potentials $U_0(\rho)$ and $U_{-1}(\rho)$ are given by Eq. (15).

It follows from Eq. (15) that in the region $\rho \gg d$,

$$U_0(\rho) = U_{-1}(\rho) \simeq -\frac{D_{eh}e^2}{4\pi\varepsilon_0\kappa\rho},$$

$$U_0(\rho) - U_{-1}(\rho) = -U_{0(-1)}(\rho)\frac{d^2}{2\rho^2} \ll U_{0(-1)}(\rho).$$

Keeping in Eqs. (43) and (44) only diagonal potentials U_0 and U_{-1}, we arrive at the function $R_0(\rho)$ [Eq. (18)] corresponding to the discrete state and the function

$$R_{-1}(\rho) = A_{-1}v^{-1/2}W_{ip/2,0}(v), \quad v = \frac{4\rho}{i\bar{a}_0 p}, \quad \mathcal{E}-\mathcal{E}_{-1} = \frac{4\overline{\mathrm{Ry}}}{p^2}, \quad (45)$$

describing the continuous state possessing the asymptote of an outgoing wave,

$$R_{-1}(\rho) = A_{-1}\exp\left[-\frac{v}{2} + \frac{1}{2}(ip-1)\ln v\right], \quad v \gg 1.$$

The quantum numbers n and p obey the relationship

$$\frac{1}{n^2}+\frac{1}{p^2}=\frac{eEd}{4\overline{\mathrm{Ry}}}. \tag{46}$$

In the region $\rho \ll d$, we take the trial function $R_0^{(0)}(\rho)$ and its first derivative $R_0^{(0)\prime}(\rho)$ according to Eqs. (19) and (20), respectively, while the function $R_{-1}^{(0)}(\rho)$ and its derivative $R_{-1}^{(0)\prime}(\rho)$ can be obtained from Eqs. (19) and (20), respectively, by replacing c_0 by c_{-1}, α_0 by α_{-1}, n by p, and u by $t=\frac{4\rho}{\bar{a}_0 p}$. Using the chosen trial functions and their first derivatives, an iteration procedure is applied by double integration of Eqs. (43) and (44) to give, in turn, for the function $R_0(\rho)$ for $u \gg \bar{g}_\sigma$

$$R_0(\rho)=c_0\left[\ln u+\alpha_0+n\left(\frac{1}{\bar{g}_0}-\frac{\alpha_0}{2}\right)u\ln u\right]+\frac{1}{2}c_{-1}\alpha_{-1}G_{01}, \tag{47}$$

with

$$G_{01}=\left[\frac{J_1(\zeta_e)}{J_0(\zeta_e)}+\frac{J_1(\zeta_h)}{J_0(\zeta_h)}\right](\bar{g}_{-1}-\bar{g}_0)=4\left[\frac{J_1(\zeta_e)}{J_0(\zeta_e)}+\frac{J_1(\zeta_h)}{J_0(\zeta_h)}\right]\frac{d}{\bar{a}_0}. \tag{48}$$

The parameters $\bar{g}_{0,-1}$ and G_{01} are calculated via Eqs. (23) and (48), respectively. The equation for the function $R_{-1}(\rho)$ for $t \gg \bar{g}_{-1}$ can be obtained from Eq. (47) by replacing u by t and the index (0) by (−1).

For $\rho \ll \bar{a}_0$, $R_0(\rho)$ is determined by Eq. (22), while $R_{-1}(\rho)$ can be obtained from Eq. (22) by replacing n by ip and u by v. A comparison between these functions and those obtained by the iteration procedure is performed. When terms of the same order are equated, we obtain the set of the two homogeneous algebraic equations for the coefficients c_0 and c_{-1}. This set is solved by the determinantal method and provides a transcendental equation for the quantum number n,

$$\left[\psi\left(\frac{1-n}{2}\right)-\frac{2}{\bar{g}_0}\right]\left[\psi\left(\frac{1-ip}{2}\right)-i\frac{\pi}{2}-\frac{2}{\bar{g}_{-1}}\right]-\frac{G_{01}^2}{\bar{g}_0\bar{g}_{-1}}=0. \tag{49}$$

Setting in Eq. (49) $n=n_0+2\chi$, $n_0=1,3,5,\ldots$, $\chi \ll 1$, $p \simeq \left(\frac{4\overline{\mathrm{Ry}}}{eEd}\right) \ll 1$, $\psi\left(\frac{1-n}{2}\right) \simeq \chi^{-1}$, we find the complex roots of Eq. (49),

$$2\chi=\bar{g}_0\left[1+\frac{G_{01}^2}{4}\left(1-i\frac{\pi\bar{g}_{-1}}{4}\right)\right],$$

and the total exciton energy $\mathcal{E}_0(n_0)$,

$$\mathcal{E}_0(n_0)=\mathcal{E}_0^{(0)}(n_0)+\Delta\mathcal{E}_0(n_0)-\frac{i}{2}\Gamma_0(n_0), \tag{50}$$

where $\mathcal{E}_0^{(0)}(n_0)$ [Eq. (38)] is the exciton energy calculated in the single-WSL approximation and

$$\Delta\mathcal{E}_0(n_0)=\frac{2\overline{\mathrm{Ry}}}{(n_0+\bar{g}_0)^3}\bar{g}_0G_{01}^2, \tag{51}$$

$$\Gamma_0(n_0)=\frac{\pi\overline{\mathrm{Ry}}}{(n_0+\bar{g}_0)^3}\bar{g}_0\bar{g}_{-1}G_{01}^2 \tag{52}$$

are the shift and the width of the exciton level both caused by the coupling of the discrete and continuous quasi-2D exciton states related to the neighboring WSLs $\sigma=0$ and $\sigma=-1$. The obtained results are valid qualitatively for arbitrary pairs of WSLs with $\Delta\sigma=\pm 1$.

Below, we describe the first approach based on the matching procedure and the Fano method[23] implying a real exciton wave function that corresponds to the continuous spectrum with real energies. This method has been originally developed in Ref. 38 and successfully applied to the resonant exciton states in a single QW. The only difference lies in the fact that in the course of the averaging, the wave functions of the isolated QW in Ref. 38 are replaced by the functions (11) at $\xi_{e,h}=0$. Since the details are provided in Ref. 38, only an outline of the calculations will be given below.

In the region $\rho \gg d$, the function (45) is replaced by the sum of the outgoing-type and incoming-type wave functions,

$$R_1(\rho)=\sqrt{\frac{m_{ex}}{\pi\hbar^2}}\exp\left(-\frac{\pi p}{4}\right)[\exp(i\Theta)v^{-1/2}W_{ip/2,0}(v)+\text{c.c.}], \tag{53}$$

where Θ is a phase.

Performing the iteration and matching procedures described above, we find the coefficient c_{-1} and the parameters $\alpha_{0,-1}=2/\bar{g}_{0,-1}$ and consequently arrive at the set of equations for the coefficients c_0 and c_{-1}. This set is solved by the determinantal method to give, in particular,

$$\varphi\left[\lambda+\frac{\pi\tan[\Theta+\sigma(p)]}{1+\exp(-\pi p)}\right]-\frac{G_{01}^2}{\bar{g}_0\bar{g}_{-1}}=0, \tag{54}$$

where

$$\varphi(n)=\psi\left(\frac{1-n}{2}\right)-\frac{2}{\bar{g}_0},\quad \lambda(p)=\frac{1}{2}\left[\psi\left(\frac{1+ip}{2}\right)+\text{c.c.}\right]-\frac{2}{\bar{g}_{-1}},\quad \sigma(p)=\arg\Gamma\left(\frac{1+ip}{2}\right).$$

The coefficient of absorption is proportional to $|R(0)|^2$, where $R(0)=R_0(0)+R_{-1}(0)\simeq 2(c_0\bar{g}_0^{-1}+c_{-1}\bar{g}_{-1}^{-1})$ [see Eq. (19)]. As a result, we arrive at the cumbersome expression that can be obtained from Eq. (54) of Ref. 38 by replacing g_{11} by $\bar{g}_{-1}$, g_{22} by $\bar{g}_0$, and g_{12} by G_{01}. The absorption described by this expression exhibits an asymmetric profile containing both resonant and antiresonant behaviors. In the vicinity of the exciton energy calculated in the single-WSL approximation [$\varphi(n)=0$, $p \ll 1$], the absorption profile is rearranged to a Lorentzian form

$$\Lambda(\omega,n_0)=\frac{\Gamma_0(n_0)}{2\pi\left\{[\mathcal{E}_0^{(0)}(n_0)+\Delta\mathcal{E}_0(n_0)-\hbar\omega]^2+\frac{1}{4}\Gamma_0^2(n_0)\right\}}, \tag{55}$$

where

$$\Gamma_0(n_0)=\frac{4\overline{\mathrm{Ry}}G_{01}^2\bar{g}_0}{(n_0+\bar{g}_0)^3\bar{g}_{-1}\lambda}\sin 2\delta, \tag{56}$$

$$\Delta\mathcal{E}_0(n_0)=-\frac{4\overline{\mathrm{Ry}}G_{01}^2\bar{g}_0}{(n_0+\bar{g}_0)^3\bar{g}_{-1}\lambda}\cos^2\delta, \tag{57}$$

and where

$$\cot\delta=\frac{\lambda}{\pi}[1+\exp(-\pi p)].$$

At $p\ll 1$, $\cos\delta\simeq 1$, $\sin\delta\simeq-\pi\bar{g}_{-1}/4$, $\lambda\simeq-2/\bar{g}_{-1}$, Eq. (56) for the resonant width and Eq. (57) for the resonant shift exactly coincide, respectively, with those for the width $\Gamma_0(n_0)$ [Eq. (52)] and the shift $\Delta\mathcal{E}_0(n_0)$ [Eq. (51)] calculated as the imaginary and real parts, respectively, of the exciton energy caused by the interwell coupling, implying the wave function of the continuous spectrum $R_{-1}(\rho)$ in the form of an outgoing-type wave [Eq. (45)].

Note that the above-mentioned complex energies of the exciton can be found by calculating the poles of the scattering matrix $S(\Theta)$ closely related to the phase shift Θ,[42]

$$S(\Theta)=\exp\{2i[\Theta+\sigma(p)]\}=\frac{\cot[\Theta+\sigma(p)]+i}{\cot[\Theta+\sigma(p)]-i}.$$

Equating the denominator to zero and using Eq. (54) at $p\ll 1$, we immediately arrive to Eq. (49) and to the complex energy levels [Eq. (50)]. Thus, the coefficient of the optical absorption induced by the transitions to the resonant exciton states can be obtained from Eq. (36) by replacing $\delta[\hbar\omega-\mathcal{E}_0^{(0)}(n_0)]$ by the Lorentzian profile $\Lambda(\omega,n_0)$ [Eq. (55)], in which $\mathcal{E}_0^{(0)}(n_0)$ is given by Eq. (38) and $\Delta\mathcal{E}_0(n_0)$ [Eq. (51)] as well as $\Gamma_0(n_0)$ [Eq. (52)] have been calculated above. We emphasize that our result is valid only in the narrow region of the photon energy of the order of $\Gamma_0(n_0)$ in the vicinity of the peak position. In order to describe the complete profile of the resonant exciton absorption, the more complicated expression similar to that derived in Ref. 38 should be taken.

V. DISCUSSION

A. Single-WSL approximation

The coefficient of the exciton absorption calculated in the single-WSL approximation $\alpha_l(\omega)$ [Eqs. (36) and (37)] reflects the exciton energy spectrum [Eq. (32)]. The optical spectrum of the exciton absorption consists of the set of quasi-Rydberg series of δ-function-type peaks ($n_0=1,3,5,\ldots$) positioned below the edge specified by the energy $\mathcal{E}_\sigma$ [Eq. (38)] overlapping with the branches of the continuous absorption associated with the $\sigma-1,\sigma-2,\ldots$ edges. Since the intensities of the exciton transitions decrease proportional to n_0^{-3}, the peak $n_0=1$ dominates other ones within each series. In the vicinity of the edge ($l\hbar\omega\leqslant\mathcal{E}_\sigma$) [Eq. (12)], the peaks with $n_0\gg 1$ are grouped together in the quasicontinuous absorption remaining finite at the edge. Above the edge ($l\hbar\omega>\mathcal{E}_\sigma$), the absorption (37) decreases and in the region $l\hbar\omega-\mathcal{E}_g\gg\mathrm{Ry}$ it is shaped into the unit step function $\Theta(l\hbar\omega-\mathcal{E}_g)$. The latter absorption is less by half than that at the edge. The peak positions are determined by the energies $\mathcal{E}_\sigma^{(0)}(n_0)$ [Eq. (38)], while the intensities within the series are different for the different numbers l of absorbed photons. The spectrum of the one-photon absorption $\alpha_1(\omega)$ [Eq. (36)] consists of three quasi-Coulomb series adjacent to the edges $\mathcal{E}_\sigma$, $\sigma=0,\pm1$. These series are separated by the frequency range $\Delta\omega=eEd/\hbar$. The intensities of the series depend on the miniband widths, period of the SL, the magnitude of the dc electric field and weakly depend on the magnitude of the ac electric field. The centrally placed series $\sigma=0$ is the most intense, whereas the relative intensities of the other ones ($\sigma=\pm1$) are of the order of $\frac{J_1^2(\zeta)}{J_0^2(\zeta)}$, resulting in about 0.2 for $\zeta=0.8$. The additional reduction of this ratio is caused by the different effect of the confinement on the $\sigma=0$ and $\sigma=\pm1$ exciton states ($\bar{g}_{\pm1}>\bar{g}_0$). The narrower the miniband widths and the larger the dc field and period, the less the intensities of the series $\sigma=\pm1$ relatively to the series $\sigma=0$ in all cases.

The employed model of the SL potential ($d_w=d$) allows us to extend our results to realistic potentials consisting of potential barriers of finite width. For the ratio d/a_0, the parameter d should be treated as the width of the QWs d_w, while for the parameters $\zeta_j\sim\frac{\Delta_j}{2eEd}$ as the period d of the SL. It follows from Eqs. (32) and (16) that the exciton binding energy $\mathcal{E}_b^{(\sigma)}$ defined as

$$\mathcal{E}_b^{(\sigma)}=\frac{4\overline{\mathrm{Ry}}}{(1+\bar{g}_\sigma)^2},\quad \overline{\mathrm{Ry}}=\mathrm{Ry}D_{eh}^2,\quad \bar{g}_\sigma\sim\frac{d_w}{a_0}D_{eh} \tag{58}$$

increases with increasing dc electric field strength. The reason for this is the fact that the electric field E reduces the effective exciton Bohr radius $\bar{a}_0=a_0D_{eh}^{-1}$. Increasing $|\sigma|$ yields an increase in the effective distance between the electron and hole $\bar{a}_0\bar{g}_\sigma$ [see, e.g., Eq. (23)], which results in a decrease of the exciton binding energy $\mathcal{E}_b^{(\sigma)}$.

The oscillator strength $I_\sigma^{(l)}$ of the intense one-photon transition ($l=1$) to the ground exciton state $n_0=1$, $\sigma=0$, ($I_0^{(1)}$) derived from Eq. (36),

$$I_0^{(1)}=\frac{D_{eh}^2J_0^2(\zeta)}{\left[1+c_0\frac{d_w}{a_0}D_{eh}\right]^3}, \tag{59}$$

and the binding energy $\mathcal{E}_b^{(0)}$ [Eq. (58)] as functions of the dc electric field E for the different GaAs/AlGaAs SLs are depicted in Fig. 1.

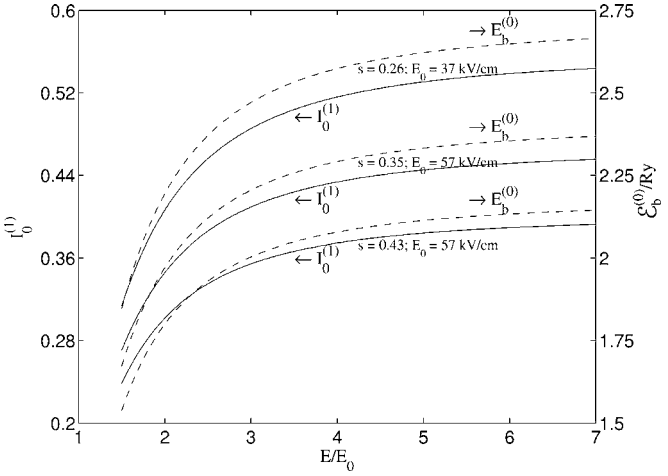

FIG. 1. The dependence of the oscillator strength $I_0^{(1)}$ [Eq. (59)] of one-photon transitions ($l=1$) to the ground exciton state $n_0=1$, $\sigma=0$ and of the binding energy $\mathcal{E}_b^{(0)}$ [Eq. (58)] on the dimensionless dc electric field E/E_0 $\left(E_0=\frac{\Delta}{2ed}\right)$ for different QW widths d_w scaled to the exciton Bohr radius a_0 ($s=d_w/a_0=0.26,0.35,0.43$) corresponding to the GaAs/AlGaAs SLs studied in Refs. 11, 22, and 18, respectively.

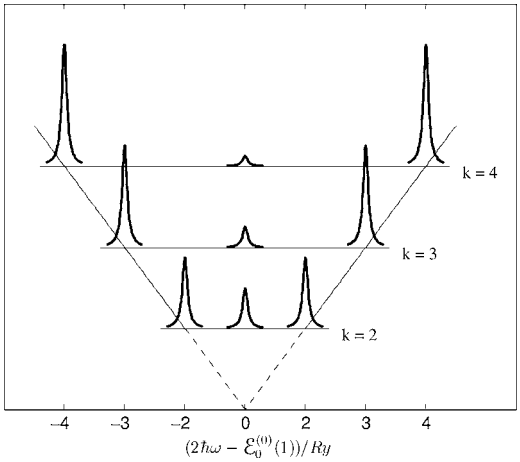

FIG. 2. The schematic form of the spectrum of the two-photon exciton absorption as a function of the shift of the photon energy $2\hbar\omega$ with respect to the peak position $\mathcal{E}_0^{(0)}(1)$ [Eq. (38)] scaled to the exciton Rydberg constant Ry for different dc electric fields E $\left(k=\frac{eEd}{\mathrm{Ry}}\right)$.

The spectrum of the multiphoton absorption [Eq. (36)] ($l=2,3,\ldots$) consists of two most intense quasi-Rydberg series adjacent to the edges $\mathcal{E}_\sigma$, $\sigma=\pm1$ and separated by the frequency interval $\Delta\omega=2eEd/\hbar l$. The corresponding multiphoton transitions arise because of the overlap of the electron (hole) time-independent term of the function $f_{e\nu}(z,t)$ [Eq. (11)] and the time-dependent terms of the hole (electron) function $f_{h\mu}(z,t)$ that, in turn, are localized within the cells $s=\nu(\mu)$ and $s=\mu\pm1(\nu\pm1)$, respectively. The intensity of the odd-photon absorption $\sim[J_0(\zeta)+J_2(\zeta)]^2$ insignificantly exceeds that of the even-photon absorption $\sim[J_0(\zeta)-J_2(\zeta)]^2$ by a factor of 1.18 at $\zeta=0.8$. In addition, the spectrum of the even-photon absorption contains the centrally placed series adjacent to the edge $\mathcal{E}_\sigma$, $\sigma=0$ of lower intensity $\sim 4J_1^2(\zeta)$. With increasing dc electric field strength (the parameter ζ_j decreases), the intensities of the main side series $\sigma=\pm1$ no longer depend on both the dc field and the parity of the number of the absorbed photons, while the peak magnitudes of the centrally placed series $\sigma=0$ become negligibly small. A sketch of the spectrum of the two-photon exciton absorption is given in Fig. 2. The intensities of the exciton peaks $\alpha_l(\omega)$, $l=1,2,\ldots$ [Eq. (36)] slowly increase with increasing dc electric field strength because of the reduction of the effective Bohr radius $\bar{a}_0$ due to the factor $\bar{a}_0^{-2}\sim D_{eh}^2(E)$ in Eq. (36). In contrast to the one-photon absorption, the ac electric field F_0 influences considerably the multiphoton transitions. The wider the miniband widths $\Delta_{e,h}$ are and the greater the magnitude F_0 is, the greater the l-photon absorption $\alpha_l \sim \left(\frac{\Delta_e+\Delta_h}{\hbar\omega}\right)^2 \gamma^{2(l-1)}$ ($\gamma<1$) is.

Figure 3 demonstrates the dependence of the oscillator strength $I_\sigma^{(l)}$ of two-photon transitions ($l=2$) to the ground exciton states ($n_0=1$, $\sigma=0,\pm1$) on the dc electric field E calculated from α_2 [Eq. (36)],

$$I_{\pm1}^{(2)}=\frac{D_{eh}^2[J_0(\zeta)-J_2(\zeta)]^2}{\left[1+c_1\frac{d_w}{a_0}D_{eh}\right]^3},\quad I_0^{(2)}=\frac{4D_{eh}^2J_1(\zeta)^2}{\left[1+c_0\frac{d_w}{a_0}D_{eh}\right]^3},\tag{60}$$

with D_{eh} from Eq. (16) and $c_{0,1}$ from Eq. (23). At this stage, we note that our analytical method implies that the corrections $\bar{g}_\sigma$ (23) to the quantum numbers $n_0=1,3,\ldots$ satisfy the conditions $\bar{g}_\sigma<1$ resulting particularly in $d_w/a_0<0.20$ for $\sigma=\pm1$. Thus, we are forced to appeal to the short-period and narrow-well GaAs/AlGaAs SL with typical parameter values

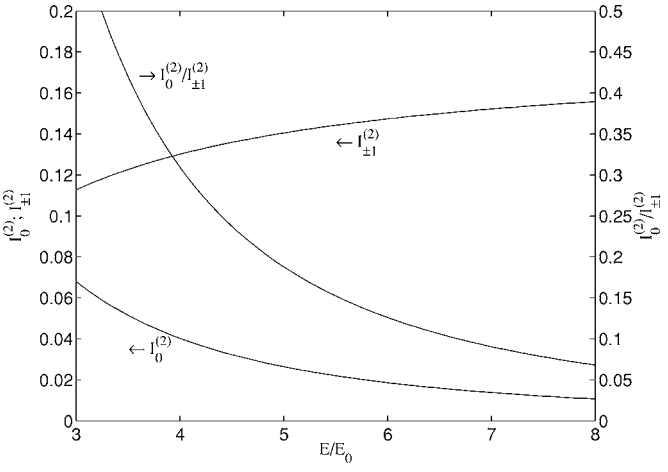

FIG. 3. The dependence of the oscillator strength $I_\sigma^{(1)}$ [Eq. (60)] of two-photon transitions ($l=2$) to the ground exciton state $n_0=1$ adjacent to the WSLs $\sigma=\pm1$ ($I_{\pm1}^{(2)}$) and $\sigma=0$ ($I_0^{(2)}$) on the dimensionless dc electric field E/E_0 $\left(E_0=\frac{\Delta}{2ed}\right)$ for the parameters of the GaAs/AlGaAs SLs (Ref. 43): $d_w=19$ Å, $d=36$ Å, $\Delta_e=193$ meV, and $\Delta_h=50$ meV.

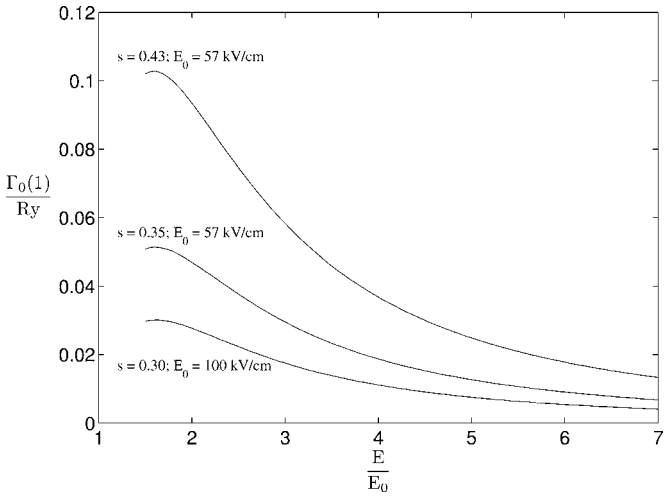

FIG. 4. The width $\Gamma_0(1)$ [Eq. (52)] of the ground exciton state $n_0=1$, $\sigma=0$ scaled to the exciton Rydberg constant Ry versus the dimensionless dc electric field E/E_0 $\left(E_0=\frac{\Delta}{2ed}\right)$ for different QW widths d_w, $s=\frac{d_w}{a_0}=0.30,0.35,0.43$ (a_0 is the exciton Bohr radius) relevant to the GaAs/AlGaAs SLs studied in Refs. 19, 22, and 18, respectively.

$d_w=19$ Å, $d_w/a_0=0.16$, $d=36$ Å, $\Delta_e=193$ meV, and $\Delta_h=50$ meV, in which the optical transitions between the WSLs were successfully observed.[43] The numerical estimates for the typical SLs of moderate periods will be given below. Figure 3 shows that with increasing dc field strength, the intensities of the main side peaks $\sigma=\pm1$ tend to a constant value, while the central weak maximum $\sigma=0$ vanishes rapidly.

B. Double-WSL approximation: Resonant width and shift

In the double-WSL approximation, the δ-function-type exciton peaks [Eq. (36)] are replaced by the peaks of a Lorentzian form [Eq. (55)] of width $\Gamma_0(n_0)$ [Eq. (52)] shifted toward larger wavelengths by an amount $\Delta\mathcal{E}_0(n_0)$ [Eq. (51)]. The resonant width $\Gamma_0(n_0)$ and the shift $\Delta\mathcal{E}_0(n_0)$ both caused by the interwell coupling associated with the dc electric field and finite widths of the QWs d_w ($d_w=d$ in our model) depend on the dimensionless parameters $\zeta_j\sim\frac{\Delta_j}{eEd}<1$ and $\frac{d_w}{a_0}<1$, respectively. The greater the dc electric field and the less the ratio $\frac{d_w}{a_0}$, the less both the shift $\Delta\mathcal{E}_0(n_0)$ and the width $\Gamma_0(n_0)$. The width $\Gamma_0(1)$ [Eq. (52)] of the ground exciton state $n_0=1$, $\sigma=0$ as a function of the dc electric field for different QW widths, relevant to the GaAs/AlGaAs SLs studied in Refs. 19, 22, and 18, is depicted in Fig. 4. Clearly, the localization (E increases) and confinement (d_w decreases) both reduce the resonant width of the exciton states. Note that the interwell coupling associated with the correction functions $\sim\lambda_j$ in Eq. (6) contributes the additional terms $\langle 0|\ldots|0\rangle$ to the matrix elements of the Coulomb potential [Eq. (15)] and consequently to the resonant shift $\Delta\mathcal{E}(n_0)$ and width $\Gamma(n_0)$. Such a contribution has the order of $(\lambda_j/\zeta_j)^2$ with respect to those determined by Eqs. (51) and (52), which, in turn, is negligibly small because of the approximation of the ground size-quantized levels b_j [Eq. (5)] being actually unperturbed by the dc electric field E $[(\lambda_j/\zeta_j)^2\sim(eEd/b_j)^2\sim\Delta b_j/b_j\ll1$, see Table I].

Also, we ignore the broadening of the exciton linewidth induced by the coupling between the bound exciton state associated with the selected WSL ($\sigma=0$) and continuous exciton states corresponding to the neighboring WSLs ($\sigma=\pm1,\ldots$). This coupling is caused by the Coulomb interaction of the electron and hole incompletely localized within the single QWs of the SL subjected to weak or moderate dc electric fields $E(eEd\leqslant\mathrm{Ry})$. This effect dominates in the region of these fields that, in turn, leads to the growth of the exciton linewidth as a function of the dc electric field.[20,46] However, in the presence of strong electric fields considered here ($eEd>\mathrm{Ry}$), the carriers become localized within one period of the SL and the mechanism described above does not contribute to the broadening of the linewidth.

In our model, the dependence of the width $\Gamma_0(n_0)$ [Eq. (52)] on the period of the SL d is determined by the factor s^4 ($s=d/a_0$) and the Bessel functions $J_\sigma(\eta_j)$, $\sigma=0,1$. The factor s^4 and the Bessel functions $J_\sigma(\zeta_j)$ describe the contribution of the 2D confinement ($s<1$) and the spatial localization ($\zeta_j<1$) to the coupling, respectively. It follows from Eq. (5) that the dependence of the miniband width Δ_j on the period d for a fixed power of the barrier β_j is given by

$$\Delta_j=\frac{\Delta_{0j}}{s^3},$$

where

$$s=\frac{d}{a_0}\quad\text{and}\quad\Delta_{0j}=\frac{2\pi^2\hbar^4}{m_j^2a_0^3\beta_j}.$$

The presented dependence of the miniband width on the period of the SL is in qualitative agreement with that found numerically in Ref. 12. The stronger dependence $\Delta_j(d)$ found in Ref. 12 is due to the fact that in this work the wells and the barriers were taken of equal width. The growth of the miniband width Δ_j is caused by the narrowing of both the wells and the barriers, while in our paper the powers of the barriers β_j are kept constant. Increasing the parameter s, the miniband-width Δ_j narrows, the localization increases, and the width $\Gamma_0(n_0)$ [Eq. (52)] decreases. On the other hand, the increase of the parameter s destroys the 2D confinement that, in turn, leads to an increase in the width $\Gamma_0(n_0)\sim s^4$ [Eq. (52)]. Thus, the localization of the carriers and 2D confinement both related to the period d are in competition, resulting in a nonmonotonic dependence of the resonant width of the exciton state on the period of the SL. This dependence calculated from Eq. (52) for the GaAs/AlGaAs SL with $\Delta_0\simeq8$ meV found from the parameters[19] $d=51$ Å, $\Delta\simeq\Delta_e\simeq100$ meV, and $a_0=115$ Å is given in Fig. 5 for different values of E. For the SL of a moderate period d ($s\geqslant0.5$, $\zeta_e\leqslant0.4$), the localization effect dominates that of the 2D confinement and the width $\Gamma_0(1)$ of the ground exciton state $n_0=1$ decreases with increasing parameter s. For the SL of smaller period d ($s\simeq0.4$, $\zeta_e\leqslant1$), the effect of the 2D confinement exceeds that of the moderate localization and the

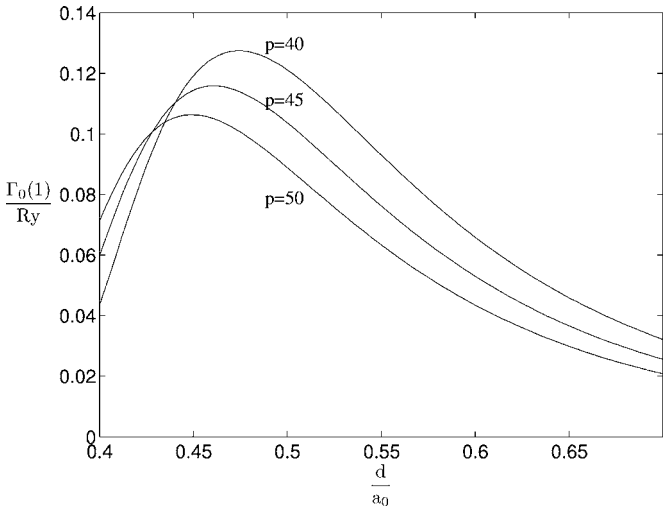

FIG. 5. The dimensionless width $\Gamma_0(1)/\mathrm{Ry}$ [Eq. (52)] (Ry is the exciton Rydberg constant) of the ground exciton state $n_0=1$, $\sigma=0$ as a function of the period of the SL d scaled to the exciton Bohr radius a_0 for different parameters $p=E/E_{ex}$ $\left(E_{ex}=\frac{\Delta_0}{2ea_0}\right)$, where $\Delta_0=8.0$ meV calculated from the parameters of the GaAs/AlGaAs SL (Ref. 19): $d=51$ Å, $\Delta_e=94.5$ meV, and $\Delta_h=5.5$ meV.

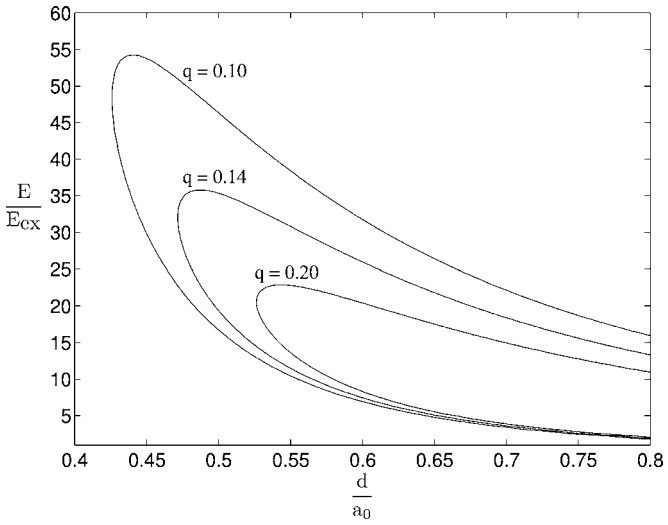

FIG. 6. Isowidth curves $\Gamma_0(1)/\mathrm{Ry}=q=\mathrm{const}$, where $\Gamma_0(1)$ [Eq. (52)] is the width of the ground exciton state $n_0=1$, $\sigma=0$, Ry and a_0 are the Rydberg constant and the Bohr radius of the exciton, respectively, d is the SL period, and E is the dc electric field scaled to the field $E_{ex}=\frac{\Delta_0}{2ea_0}$, $\Delta_0=8.0$ meV (see Fig. 5 caption for details).

width $\Gamma_0(1)$ increases with increasing parameter s. In this region, the dependence of the resonant width on the dc electric field deviates from that corresponding to moderate periods. The reason is that the chosen electric fields become inadequately large to provide a considerable localization for the short-period SLs because of wide minibands. The analogous situation has been revealed numerically for relatively weak electric fields.[46] The isowidth curves reflecting the relationships between the field E and period d at which the width $\Gamma_0(1)$ [Eq. (52)] of the ground exciton state ($n_0=1$, $\sigma=0$) remains constant are shown in Fig. 6 for the parameters of the SL mentioned above.[19]

The exciton peaks associated with the transitions to the excited states $n_0=3,5,\ldots$ are much narrower $[\Gamma_\sigma(n_0)\sim n_0^{-3}]$ and much less shifted $[\Delta\mathcal{E}_\sigma(n_0)\sim n_0^{-3}]$ compared to those corresponding to the ground state $n_0=1$. It seems that only the ground exciton peak $n_0=1$ can be experimentally resolved.

C. Criteria of the approximations

Let us turn to the relationships between the modern experimental and theoretical studies for GaAs/AlGaAs SLs in electric fields and the approximations applied here.

In Table I, we present the parameters providing the quasi-2D character of the exciton states ($d_w/a_0 \ll 1$), restriction by the ground electron and hole minibands only ($w_{e,h} \ll 1$ and $\Delta b_{e,h}/b_{e,h} \ll 1$), localization of the carriers within the one period d ($E_0/E \ll 1$), and the double-WSL approximation ($4\ \mathrm{Ry}/eEd \ll 1$). In the above conditions, d_w is the width of the QWs, $w_{e,h}(F_0,\omega)$ is the probability of the interminiband transitions caused by the ac electric field $F_0\cos\omega t$, and $\Delta b_{e,h}(E)$ is the correction to the size-quantized ground level $b_{e,h}$ induced by the dc electric field E. We also estimate the widths of the exciton levels associated with the coupling between the ground and first excited minibands in the presence of the dc electric field (Zener tunneling) ($\Gamma_{e,h}^{Zener}$). The parameter $\gamma=eF_0d/\hbar\omega$ ($\gamma<1$) and the probabilities $w_{e,h}$ are calculated for the electric field $F_0=340$ kV/cm and the frequency ω ($\hbar\omega=750$ meV) relevant to the two-photon absorption emanated by a 2 MW Er laser focused on a spot with diameter 700 μm. For the parameters of the GaAs material, we take $m_e=0.067m_0$, $m_{hh}=0.62m_0$, $\mu=0.060m_0$, $\varepsilon=13.2$, Ry=4.7 meV, and $a_0=115$ Å.[44] We limit ourselves to heavy-hole excitons and neglect the valence-band mixing and contribution of the light-hole excitons which are well justified for structures composed of relatively narrow QWs.[19]

It follows from the data and references provided in Table I that all existing studies refer to the case of a narrow QW ($d_w<a_0$). For the estimates of the probability of the transition between the ground and first excited electron minibands induced by the ac electric field $w_e(F_0,\omega)$, we have

$$w_e(F_0,\omega)\sim\frac{|eF_0z_{12}|^2}{2}\left[\frac{1}{(\hbar\omega-\Delta b_e)^2}+\frac{1}{(\hbar\omega+\Delta b_e)^2}+\frac{1}{(\hbar\omega-\Delta b_e)(\hbar\omega+\Delta b_e)}\right],$$

where $z_{12}\sim\frac{d_w}{5}$ is the matrix element of the z coordinate calculated with respect to the electron wave functions of the ground and first excited size-quantized states and $\Delta b_e=3b_e$ is the gap between the ground (b_e) and first excited size-quantized levels. The correction $\Delta b_h(E)$ to the ground hole size-quantized level $b_h=\frac{\hbar^2\pi^2}{2m_hd_w^2}$ caused by the dc electric field E reads

$$\Delta b_h(E)\sim\frac{(eEd_w)^2}{\pi^4b_h}.$$

TABLE I. The QW widths d_w, periods d, electron-hole miniband widths $\Delta=\Delta_e+\Delta_{hh}$, the dc electric fields E, corrections $\Delta b_e(E)$ to the ground size-quantized electron energy levels b_e, probabilities w_e of the interlevel transitions induced by the ac electric field $F_0=340$ kV/cm, $\hbar\omega=750$ meV, the widths of the exciton levels Γ^{Zener} caused by the intersubband Zener tunneling, and the parameter $\gamma=eF_0d/\hbar\omega$ corresponding to the GaAs/AlGaAs SLs studied in Refs. 8, 19, 20, 22, and 18. The Bohr radius a_0 and the Rydberg constant Ry of the exciton are taken to be $a_0=115$ Å and Ry=4.7 meV (Ref. 44). The miniband widths * and ** are estimated from the Refs. 34 and 10, respectively.

	Ref. 8	Ref. 19	Ref. 20	Ref. 22	Ref. 18
d_w (Å)	45	34	67	41	50
d (Å)	90	51	84	65	65
E (kV/cm)	11	25	25	40	50
Δ (meV)	11.2	100*	35	75**	75
d_w/a_0	0.39	0.29	0.58	0.35	0.43
E_0 (kV/cm)	6.2	98.0	20.8	57.6	67.6
$4\mathrm{Ry}/eEd$	1.9	1.48	0.89	0.72	0.58
γ	0.40	0.22	0.37	0.29	0.29
$w_e(F_0,\omega)$	0.5	8.6×10^{-4}	5.9×10^{-3}	5.1×10^{-2}	4.5×10^{-2}
$\Delta b_h/b_h$	3.9×10^{-4}	2.7×10^{-4}	2.3×10^{-2}	3.0×10^{-3}	1.5×10^{-2}
Γ_h^{Zener} (meV)			1.1×10^{-4}		2.9×10^{-5}

Since the probability of the interminiband electron transitions $w_e(F_0,\omega)\ll1$ and correction to the ground hole size-quantized level are negligibly small ($\Delta b_h(E)\ll b_h$), the interminiband transitions induced by both the ac and the dc electric fields can be neglected. The probability of the hole transitions $w_h(F_0,\omega)$ and relative correction to the electron size-quantized ground level $[\Delta b_e(E)/b_e]$ are both less than $w_e(F_0,\omega)$ and $(\Delta b_h(E)/b_h)$, respectively. The reason for the significant probability $w_e(F_0,\omega)\simeq0.5$ (Ref. 8) is the fact that for the parameters of the SL taken in Ref. 8, the chosen photon energy $\hbar\omega=750$ meV is in resonance with the first electron miniband gap. However, for the SL of the same parameters the interminiband probability for the photon energy relevant to the three-photon absorption is found to be $w_e(F_0,\omega)\simeq1.8\times10^{-2}\ll1$. Thus, we can focus on the ground electron and hole minibands.

The width of the resonant states Γ_h^{Zener} associated with the Zener tunneling between the ground and first excited hole minibands calculated via Ref. 45,

$$\Gamma_h^{Zener}=\frac{eEd}{2\pi}\exp\left[-\frac{m_hd(\Delta b_{12,h})^2}{4\hbar^2eE}\right], \tag{61}$$

is negligibly small (see Table I). In Table I, the widths Γ_h^{Zener} are given only for the SLs studied in Refs. 20 and 18. The widths Γ_h^{Zener} calculated for the SLs investigated in the remaining references are much smaller than those presented in Table I. The width of the ground exciton resonance estimated according to Eq. (52) for the only SL (Ref. 8) providing more or less localized excitons ($E_0<E$) in a relatively narrow QW ($d_w<a_0$) gives the result $\Gamma_0(1)\simeq0.54$ meV. Note that $\Gamma_e^{Zener}\ll\Gamma_h^{Zener}$ and thus we conclude that for the cases treated in the references of Table I both resonant and nonresonant miniband couplings have a minor effect.

In an effort to demonstrate that relatively strong electric fields $E>E_0$ provide the monotonic dependencies excluding the unexpected phenomena in Figs. 1 and 3–5, we extended the dc fields to the values $E\simeq7E_0$. In spite of the significant absolute values of these fields, the theoretical probability of the Zener intersubband tunneling determined by the exponential factor in Eq. (61) remains small (3.2×10^{-2}–10^{-10}). The relatively narrow QWs considered here prevent the SL from the electric breakdown. Only in the case of (Ref. 18, Fig. 1) the limiting dc field $E=7E_0$ is less but close to the threshold field. Note that usually the experimental critical fields are less than those calculated theoretically. The maximum dc electric fields related to Fig. 5 and Ref. 11 (Fig. 1) contribute to the Zener width a negligibly small amount of the order of 10^{-6}–10^{-9} meV, while for the remaining cases (Ref. 22 in Fig. 1, Ref. 43 in Fig. 3, and Ref. 19 in Fig. 4) this contribution is about 0.1–1.3 meV. In the latter cases, in order to ignore the Zener tunneling the limitation of the dc electric fields by the condition $E\leqslant(2-3)E_0$ is desirable. Above these fields, the effect of the intersubband Zener transitions on the interwell WSL coupling should be taken into account.[8]

References 8 and 20 deal with the situation where carriers are localized by the dc electric field within one period of the SL ($E_0/E<1$). For the remaining references, the relatively weak dc electric fields prevent the carriers to be effectively localized. However, in the presence of a dc electric field of strength $E=72$ kV/cm (see Refs. 18 and 22) and $E=125$ kV/cm for Ref. 19, the ratio E_0/E becomes equal to about 0.8. In the presence of the dc electric fields of Refs. 18, 20, and 22, the binding energy of the quasi-2D excitons (4 Ry) is less than the distance between the neighboring WSLs (eEd) ($4\ \mathrm{Ry}/eEd<1$). For the electric field $E=30$ kV/cm applied to the SL considered in Ref. 8 and $E=50$ kV/cm in Ref. 19, the parameter $4\ \mathrm{Ry}/eEd$ becomes 0.60 and 0.75, respectively, and the corresponding quasi-2D

exciton series is associated with the corresponding WSL (single- and double-WSL approximations). Clearly, the relatively strong dc electric fields considered in this work provide the spectrum of the exciton absorption convenient for the experimental study because the Rydberg series are separated. In other case of the moderate and weak fields $eEd \leqslant \Delta$, 4 Ry optical spectrum would constitute the sequence of the superimposed exciton series adjacent to a number of the WSLs $\sigma=0,\pm1,\pm2,\ldots$. In all cases given in Table I, the parameter $\gamma=eF_0d/\hbar\omega$ satisfies the condition $\gamma<1$. This allows the conclusion that the parameters of the studies reflected in Table I meet those used in this work or are at least close to them. Thus, all employed approximations, namely, the narrow-well SLs ($d_w/a_0 \ll 1$), neglecting the coupling between the ground and excited minibands [$w_{e,h}(F_0,\omega) \ll 1$, $\Delta b_{e,h}(E)/b_{e,h} \ll 1$] and interminiband Zener tunneling ($\Gamma_{e,h}^{Zener} \ll \Gamma_0$), localization of the carriers ($E_0 \ll E$), single- and double-WSL approximations (4 Ry $\ll eEd$), as well as the condition $\gamma<1$, are in line with the current experimental and theoretical studies and are therefore well justified.

D. Comparison with other methods and experiment

Our analytical results are in agreement with those obtained by numerical studies and with the available experimental data. Though we do not focus here on the one-photon absorption, we note that its signatures, i.e., linear increase of the distance between the exciton peaks $\sigma=0,\pm1$ and corresponding decrease of the oscillator strengths of the peaks $\sigma=\pm1$ relative to the peak $\sigma=0$ with increasing dc electric field observed in Refs. 9–14, are reflected in Eq. (36). In these papers, both the above listed signatures and others are well represented in the corresponding figures and diagrams. The dependencies of the binding energy of the exciton associated with the WSL $\sigma=0$ and corresponding oscillator strengths on the dc electric field (Fig. 1) correlate well with the results of the numerical calculations of Leavitt and Little up to $E_{max}=70$ kV/cm (Ref. 11) and of Dignam and Sipe up to $E_{max}=140$ kV/cm (Ref. 13). For the binding energy presented in Ref. 11, the discrepancy within the interval $E=50-70$ kV/cm ($E_0=37$ kV/cm) does not exceed 11%. The same holds for the binding energy obtained by Dignam and Sipe for $E=100$ kV/cm ($E_0=57$ kV/cm), while as expected for the electric field $E=140$ kV/cm the difference is about 1.5%. The quantitative deviations of our oscillator strengths (Fig. 1) from those calculated in Refs. 11 and 13 are caused by the different definitions of it. In particular, Leavitt and Little pointed out that they ignored the dependence of the oscillator strength on the reciprocal exciton Bohr radius a_0^{-1} providing the additional dependence on the dc electric field, while in our approach this dependence $\sim a_0^{-1}D_{eh}$ [see eq. (16) for D_{eh}] is taken into account.

In Refs. 46 and 20, the experimental spectrum consisting of exciton resonances in biased GaAs/AlGaAs SLs has been compared to the numerical calculations derived from the theories based on the Green's function method[46] and on the Born-Markov equations of a SL.[20] It was found that the widths $\Gamma_\sigma(1)$ of the ground exciton peaks $n_0=1$ relevant to the WSLs $\sigma=0,\pm1$ decrease with increasing dc electric field E with $\Gamma_{\pm1}(1)<\Gamma_0(1)$. This correlates completely with our results (see Fig. 4). In particular, extending Eq. (52) for $\Gamma_0(1)$ to $\Gamma_1(1)$, we expect that

$$\Gamma_1(1) \sim \frac{\overline{\mathrm{Ry}}}{(1+\bar{g}_1)^3}\bar{g}_1\bar{g}_0(\bar{g}_1-\bar{g}_0)^2 \quad \text{with} \quad \frac{\Gamma_1(1)}{\Gamma_0(1)} \simeq \frac{(1+\bar{g}_0)^3}{(1+\bar{g}_1)^3} < 1$$

as $\bar{g}_0<\bar{g}_1$ [see Eq. (23)]. Relatively wide QWs of width 67 Å ($d_w/a_0=0.58$) and insufficiently strong dc electric field considered in Refs. 46 and 20 ($E_{max}=33$ kV/cm, while $E_0=21$ kV/cm) prevent us from a quantitative comparison of our results and those given in Ref. 46.

Since a dc electric field E has not been imposed on the SLs studied in Refs. 26–30 on two- and three-photon spectroscopy and since to our knowledge the experimental study of multiphoton electroabsorption in SLs has not been widely addressed in the literature to date, we estimate the values expected in a possible experiment. Estimates are now made for the recently studied[19] GaAs/$Al_{0.3}Ga_{0.7}As$ SL of period $d=51$ Å formed by the QWs of width $d_w=34$ Å separated by the barriers of width 17 Å with the bandwidth $\Delta \simeq 100$ meV estimated from Ref. 34. The exciton Rydberg Ry, the exciton Bohr radius a_0, and the magnitude F_0 and the frequency ω of the ac electric field of the laser wave are Ry=4.7 meV, $a_0=115$ Å, $F_0=340$ kV/cm, and $\hbar\omega \simeq 750$ meV. For the dc electric field E, providing the spatial localization of the exciton, we take $E=180$ kV/cm. For the chosen structure and the characteristics of the electric fields, the parameters relevant to the coefficient of two-photon absorption α_2 [Eq. (36)] become $\xi=0.13$, $\gamma=0.23$, $Q_2=0.03$, and $\zeta=0.55$. This allows us to estimate the ratio of the intensities of the main peaks $\sigma=\pm1$ of two-photon absorption to that of one-photon absorption $\sigma=0$ as

$$\frac{\alpha_2}{\alpha_1} \sim (\xi Q_2)^2\left[\frac{\mathcal{E}_b^{(0)}(E)}{\mathcal{E}_b^{(\pm1)}(E)}\right]^{3/2},$$

where $\mathcal{E}_b^{(\sigma)}(E)$ are the binding energies [Eq. (58)] of the excitons associated with the σ WSLs. Equation (58) implies that $\bar{g}_\sigma<1$. It follows from Eq. (23) that for the chosen well width d_w (equal to d in our model), the above condition is valid only for $\sigma=0$. In an effort to estimate the ratio α_2/α_1, we take the ratio of the binding energies from Ref. 11. In this work, the binding energies were calculated numerically for the correlated SL of period $d=2d_w=60$ Å, for the wide region of the electric fields E to give, in turn, for the relatively strong dc field E ($\zeta<1$) the results $\mathcal{E}_b^{(0)}/\mathcal{E}_b^{(\pm1)} \simeq \text{const} \simeq 1.7$ and $\alpha_2/\alpha_1 \simeq 3.6\times10^{-5}$. This leads one to expect that the discussed two-photon absorption can be detected experimentally similar to that observed in the ZnSe/ZnSSe SL of the correlated parameters for which the significantly smaller ratio $\alpha_2/\alpha_1 \simeq 6\times10^{-7}$ occurs.[29]

The ratio of the intensity of the weak central peak $\sigma=0$ ($\alpha_{2,0}$) to that of the main side peaks $\sigma=\pm1$ ($\alpha_{2,\pm1}$) estimated in the same manner yields

$$\frac{\alpha_{2,0}}{\alpha_{2,\pm 1}} \sim \frac{4J_1^2(\zeta)}{[J_0(\zeta)-J_2(\zeta)]^2}\left[\frac{\mathcal{E}_b^{(0)}(E)}{\mathcal{E}_b^{(\pm 1)}(E)}\right]^{3/2} \simeq 0.75.$$

It follows from Eq. (36) that the distance between the central and side peaks of the two-photon absorption is about 90 meV, while the main side peaks are separated by an amount of 180 meV. The width of the $\sigma=0$ central exciton peak estimated from Eq. (52) is found to be $\Gamma_0(1) \simeq 0.15$ meV. Taking into account that the widths of the main side peaks obey $\Gamma_{\pm 1}(1) < \Gamma_0(1)$,[46] we conclude that the resonant coupling between the different WSLs does not prevent the experimental observation of the multiphoton exciton maximum in the strongly biased short-period SLs formed by narrow QWs.

The light polarization dependence of two-photon exciton absorption in multi-quantum-well structures has been studied in Ref. 30. Based on this paper, we expect that multiphoton exciton electroabsorption for the ac electric field polarized in the heteroplanes (s polarization) would consist of discrete peaks and a continuous spectrum of different intensities and forms with respect to the case of the ac field polarized parallel to the SL axis (p polarization) considered here. The standard experimental configuration implies the radiation directed at angle to the heteroplanes that, in turn, leads to the imposition of differently polarized spectra.[27] The contributions of spectra depend on the direction of radiation. For the light wave directed parallel (perpendicular) to the SL axis, we arrive at the $s(p)$-polarized spectrum. The latter requires multiperiod SLs. The angular dependence allows, in principle, the separation of the absorption of light polarized differently. The photoluminescence excitation technique has been used applying a selective polarization configuration to study the two-photon absorption in multi-quantum-well structures.[30]

The resonant states of the Coulomb particle in the biased SL are analogous to those in bulk material in the presence of a strong magnetic field $\mathbf{B}$,[47,48] providing the effective two-dimensional confinement in the plane perpendicular to the magnetic field $\mathbf{B}$ bounded by the magnetic length $a_B = (\hbar/eB)^{1/2}$. The resonance comes from the coupling of the one-dimensional quasi-Rydberg and extended Coulomb states, each associated with the different equidistant Landau subbands. The investigations of these diamagnetic resonant states based on the theory of Fano[23] were undertaken in Refs. 49–51, whereas the multisubband approximation was employed in Refs. 52 and 53. Our results derived for the resonant exciton states in the biased SL are in complete qualitative agreement with those corresponding to the diamagnetic resonant exciton states in bulk material.[49–53] The resonant shift and width both decrease with the increase of the confinement, i.e., with the decrease of the width d of the QWs and with the increase of the dc electric field E for the biased SL and with the increase of the magnetic field B for the bulk material.

In the case of anisotropic energy bands with effective masses $m_{\|,\perp j}$ $(j=e,h)$ corresponding to the motion parallel and perpendicular to the SL z axis, respectively, the exciton states depend on the ratio $m_{\perp j}/m_{\|j}$ that, in principle, requires a numerical study. In a narrow QW ($d < a_0$), the in-plane motion is governed by the Coulomb potential and the effective mass $m_{\perp j}$, while the mass $m_{\|j}$ determines the z states. This allows us to obtain the final results for the exciton peak position and for the resonant shifts and widths of the exciton states by the following replacements. In Eqs. (36), (37), (51), (52), (38), and (5), $\bar{a}_0$ is replaced by $\bar{a}_0 \frac{m_{ex}}{m_{ex\perp}}$, $\overline{\mathrm{Ry}}$ by $\overline{\mathrm{Ry}} \frac{m_{ex\perp}}{m_{ex}}$, $\overline{g_\sigma}$ by $\overline{g_\sigma} \frac{m_{ex\perp}}{m_{ex}}$, where $m_{ex\perp}^{-1} = m_{e\perp}^{-1} + m_{h\perp}^{-1}$, b_j by $b_j \frac{m_j}{m_{j\|}}$, and Δ_j by $\Delta_j \frac{m_j}{m_{j\|}}$, $j=e,h$.

For a more realistic model of the QW of finite depth having the z-dependent effective masses $m_{\|eh}(z)$, the wave functions $u_s(z_j)$ [Eq. (6)] should be replaced by those relevant to the mentioned properties.[44]

For the QWs of intermediate width comparable to the exciton Bohr radius, the states of the first excited electron and hole minibands should be taken under consideration at least. For the moderate strengths of the dc electric field E for which the distance between the neighboring WSLs eEd becomes of the order of the 2D exciton binding energy 4 Ry, the single- and the double-WSL approximations become inappropriate. Nevertheless, the resonant states can be found in the multi-WSL approximation. Only at the final stage of the determinantal procedure is some minor numerical study necessary. We expect that in the multisubband approximation, the series (40) is rapidly convergent as happens with the series describing the diamagnetic resonant states.[53] However, these states demonstrate that the multi-Landau subband approximation[53] does not lead to significant qualitative changes relative to the two-subband model.[52] For the SLs with relatively narrow potential barriers of width ~ 20 Å,[10,21,43] the dispersion law becomes different from Eq. (5) calculated in the nearest-neighbor tight-binding approximation. In this case, our results may be applied only qualitatively.

VI. CONCLUSION

We have developed an analytical approach to the problem of multiphoton absorption in the narrow-well SLs induced by the optical transitions to the resonant exciton states spatially localized by the dc electric field. The dc electric field and the ac electric field of the intense laser wave are both directed parallel to the SL axes. The resonant character is caused by the coupling of the exciton states of the discrete and continuous spectra adjacent to the neighboring Wannier-Stark levels. The SL potential is modeled by the periodic chain of the QWs separated by the weakly penetrated δ-function-type barriers providing the validity of the nearest-neighbor tight-binding approximation. The dependencies of the coefficient of the multiphoton exciton absorption upon the characteristics of the ac and dc electric fields and parameters of the SL are obtained in an analytical form. The most intense optical quasi-Rydberg series consisting of peaks of finite resonant width are those adjacent to the WSLs with the indexes $\sigma = \pm 1$. The wider the miniband widths and the larger the amplitude of the ac electric field, the larger the intensity of the multiphoton absorption. Narrowing the SL QWs and increas-

ing the dc electric field lead in all cases to a decrease of the resonant width and shift of the exciton states. The approximations employed in this work correspond to the characteristics of the ac and the dc electric fields and the parameters of the SL chosen for recent experimental and theoretical studies (see Table I). Our analytical results are in line with those calculated numerically. Estimates of the expected experimental values made for the parameters of the GaAs/AlGaAs SL show that the multiphoton exciton absorption in biased SL should be observable experimentally.

ACKNOWLEDGMENTS

The authors are grateful to V. Bezchastnov for valuable discussions and to D. Buchholz as well as to I. Solov'ev for technical assistance. B.S.M. thanks the Deutsche Forschungsgemeinschaft for financial support.

[1] F. Bloch, Z. Phys. **52**, 555 (1928).
[2] G. H. Wannier, Phys. Rev. **117**, 432 (1960).
[3] D. H. Dunlap and V. M. Kenkre, Phys. Rev. B **34**, 3625 (1986).
[4] X.-G. Zhao, Phys. Lett. A **167**, 291 (1992).
[5] J. Zak, Phys. Rev. Lett. **71**, 2623 (1993).
[6] X.-G. Zhao, R. Jahnke, and Q. Niu, Phys. Lett. A **202**, 297 (1995).
[7] W.-X. Yan, S.-Q. Bao, X.-G. Zhao, and J.-Q. Liang, Phys. Rev. B **61**, 7269 (2000).
[8] K. Yashima, K. Hino, and N. Toshima, Phys. Rev. B **68**, 235325 (2003).
[9] E. E. Mendez, F. Agulló-Rueda, and J. M. Hong, Phys. Rev. Lett. **60**, 2426 (1988).
[10] F. Agulló-Rueda, E. E. Mendez, and J. M. Hong, Phys. Rev. B **40**, 1357 (1989).
[11] R. P. Leavitt and J. W. Little, Phys. Rev. B **42**, 11784 (1990).
[12] D. M. Whittaker, Phys. Rev. B **41**, 3238 (1990).
[13] M. M. Dignam and J. E. Sipe, Phys. Rev. B **43**, 4097 (1991).
[14] N. Linder, Phys. Rev. B **55**, 13664 (1997).
[15] J. M. Lachaine, M. Hawton, J. E. Sipe, and M. M. Dignam, Phys. Rev. B **62**, R4829 (2000).
[16] M. M. Dignam and M. Hawton, Phys. Rev. B **67**, 035329 (2003).
[17] A. Zhang, L. Yang, and M. M. Dignam, Phys. Rev. B **67**, 205318 (2003).
[18] A. Zhang and M. M. Dignam, Phys. Rev. B **69**, 125314 (2004).
[19] K.-I. Hino, K. Goto, and N. Toshima, Phys. Rev. B **69**, 035322 (2004).
[20] C. P. Holfeld, W. Schäfer, and K. Leo, Phys. Rev. B **68**, 125325 (2003).
[21] L. Yang, B. Rosam, J.-M. Lachaine, K. Leo, and M. M. Dignam, Phys. Rev. B **69**, 165310 (2004).
[22] M. Pacheco and Z. Barticevic, Phys. Rev. B **64**, 033406 (2001).
[23] U. Fano, Phys. Rev. **124**, 1866 (1961).
[24] M. Glück, A. R. Kolovsky, and H. J. Korsch, Phys. Rep. **366**, 103 (2002).
[25] J. R. Madureira, P. A. Schulz, and M. Z. Maialle, Phys. Rev. B **70**, 033309 (2004).
[26] I. M. Catalano, A. Cingolani, R. Cingolani, M. Lepore, and K. Ploog, Phys. Rev. B **40**, 1312 (1989).
[27] R. Tommasi, M. Lepore, M. C. Netti, I. M. Catalano, and I. Suemune, Phys. Rev. B **49**, 14367 (1994).
[28] M. Lepore, A. Adinolfi, M. C. Netti, I. M. Catalano, and I. Suemune, Nuovo Cimento D **18D**, 465 (1996).
[29] M. Lepore, A. Adinolfi, M. C. Netti, I. Catalano, and I. Suemune, J. Phys.: Condens. Matter **9**, 7667 (1997).
[30] A. Adinolfi, M. C. Netti, M. Lepore, F. Minerva, and I. M. Catalano, J. Phys.: Condens. Matter **10**, 9173 (1998).
[31] T. Meier, G. von Plessen, P. Thomas, and S. W. Koch, Phys. Rev. Lett. **73**, 902 (1994); Phys. Rev. B **51**, 14490 (1995).
[32] V. M. Axt, G. Bartels, and A. Stahl, Phys. Rev. Lett. **76**, 2543 (1996).
[33] M. Dignam, J. E. Sipe, and J. Shah, Phys. Rev. B **49**, 10502 (1994).
[34] A. G. Zhilich, Sov. Phys. Solid State **34**, 1875 (1992).
[35] B. S. Monozon, A. G. Zhilich, C. A. Bates, and J. L. Dunn, J. Phys.: Condens. Matter **6**, 10001 (1994).
[36] B. S. Monozon, J. L. Dunn, and C. A. Bates, Phys. Rev. B **50**, 17097 (1994).
[37] B. S. Monozon, J. L. Dunn, and C. A. Bates, J. Phys.: Condens. Matter **8**, 877 (1996).
[38] B. S. Monozon and P. Schmelcher, Phys. Rev. B **71**, 085302 (2005).
[39] *Handbook of Mathematical Functions*, edited by M. Abramowitz and I. A. Stegun (Dover, New York, 1972).
[40] Al. L. Efros, Sov. Phys. Semicond. **20**, 808 (1986).
[41] R. J. Elliot, Phys. Rev. **108**, 1384 (1957).
[42] R. G. Newton, *Scattering Theory of Waves and Particles*, 2nd ed. (Springer, New York, 1982).
[43] R. P. Leavitt and J. W. Little, Phys. Rev. B **41**, 5174 (1990).
[44] P. Harrison, *Quantum Wells, Wires and Dots* (Wiley, New York, 2000), p. 183.
[45] S. Glutsch, F. Bechstedt, B. Rosam, and K. Leo, Phys. Rev. B **63**, 085307 (2001).
[46] C. P. Holfeld, F. Löser, M. Sudzius, K. Leo, D. M. Whittaker, and K. Köhler, Phys. Rev. Lett. **81**, 874 (1998).
[47] R. J. Elliott and R. Loudon, J. Phys. Chem. Solids **15**, 196 (1960).
[48] H. Hasegawa and R. E. Howard, J. Phys. Chem. Solids **21**, 179 (1961).
[49] B. S. Monozon and A. G. Zhilich, Sov. Phys. Semicond. **2**, 150 (1968).
[50] S. D. Beneslavskii, Sov. Phys. Solid State **10**, 2503 (1969).
[51] E. I. Rashba and V. M. Edelstein, Sov. Phys. JETP **31**, 765 (1970).
[52] A. G. Zhilich and O. A. Maksimov, Sov. Phys. Semicond. **9**, 616 (1975).
[53] A. G. Zhilich and B. K. Kyuner, Sov. Phys. Semicond. **15**, 1108 (1981).